DISCLAIMER

This report was prepared as an account of work sponsored by an agency of the United States Government. Neither the United States Government nor any agency thereof, nor any of their employees, makes any warranty, express or implied, or assumes any legal liability or responsibility for the accuracy, completeness, or usefulness of any information, apparatus, product, or process disclosed, or represents that its use would not infringe privately owned rights. Reference herein to any specific commercial product, process, or service by trade name, trademark, manufacturer, or otherwise does not necessarily constitute or imply its endorsement, recommendation, or favoring by the United States Government or any agency thereof. The views and opinions of authors expressed herein do not necessarily state or reflect those of the United States Government or any agency thereof. Reference herein to any social initiative (including but not limited to Diversity, Equity, and Inclusion (DEI); Community Benefits Plans (CBP); Justice 40; etc.) is made by the Author independent of any current requirement by the United States Government and does not constitute or imply endorsement, recommendation, or support by the United States Government or any agency thereof.

Final Technical Report (FTR)

Cover Page

a. Federal Agency	Department of Energy	
b. Award Number	DE-EE0009269 WBS#: 2.3.4.609	
c. Project Title	Synergistic Thermo-Microbial-Electrochemical (T-MEC) Approach for Drop-In Fuel Production from Wet Waste	
d. Recipient Organization	Princeton University	
e. Project Period	Start: Oct 1, 2020 (signed April 1, 2021)	End: Sept. 30, 2024
f. Principal Investigator (PI)	Name: Z. Jason Ren, Title: Professor Email: zjren@princeton.edu, Phone: 609-258-7580	
g. Business Contact (BC)	Name: Anne Ochiai Title: Sr. Grant and Contract Administrator Email: anneochiai@princeton.edu Phone: 609-258-2813	
h. Teaming Partners	Pacific Northwest National Laboratory University of Illinois Urbana-Champaign	

1. Acknowledgement:

This material is based upon work supported by the U.S. Department of Energy's Office of Energy Efficiency and Renewable Energy (EERE) Bioenergy Technologies Office (BETO) under the [DE-FOA-0002203: FY20 Bioenergy Technologies Multi-Topic FOA] Award Number(s) [DE-EE0009269].

2. Disclaimer:

3. Executive Summary:

This project successfully developed and demonstrated the synergistic thermo-microbial-electrochemical (T-MEC) process, converting food waste into sustainable biofuels while achieving self-sustaining wastewater treatment and hydrogen production. By integrating hydrothermal liquefaction (HTL) and microbial electrolysis cells (MECs), the project advanced waste-to-fuel technology and expanded the understanding of sustainable waste valorization. It established a scalable framework for achieving high carbon efficiency, effective pollutant removal, and energy recovery, showcasing the potential of combining biological, thermal, and electrochemical systems to optimize resource recovery and reduce environmental impacts.

The project demonstrated the technical effectiveness of the T-MEC process, achieving over 50% improvement in carbon efficiency and reducing waste processing costs by more than 25% compared to anaerobic digestion (AD). The HTL pilot reactor processed food waste at 90 kg/h, producing up to 200 L/day of biocrude oil with high conversion efficiency. A critical desalting step in pretreatment prevented catalyst fouling, enabling efficient hydrotreating with 100% deoxygenation and denitrogenation and sulfur reduction to <15 ppm. This positioned the kerosene fraction as a strong candidate for sustainable aviation fuel (SAF). The MECs achieved rapid startup, 86.4% COD removal, and hydrogen production rates of 1.8 L H_2/L_{cat}/day, among the highest recorded for pilot-scale systems. The integrated process achieved 65% carbon efficiency to biocrude and 58% to finished fuels, outperforming AD's 41% and 33% efficiencies for biogas and natural gas vehicle fuels. System analysis highlighted economic potential, with minimum fuel selling prices (MFSP) decreasing from $25/GGE at 5 tpd to $10/GGE at 500 tpd due to economies of scale. Future work will focus on reducing MEC material and membrane costs, enhancing performance through higher current densities, and creating tailored operational strategies for diverse feedstocks. Optimization of the integrated system will improve scalability and feasibility, positioning the T-MEC process as a competitive solution for converting wet waste into sustainable fuels and clean water.

Beyond its technical and economic achievements, the project offers significant public benefits. The T-MEC process provides a sustainable alternative to landfilling and incineration, reducing greenhouse gas emissions and conserving resources. Converting waste into SAF and renewable fuels supports decarbonization in the transportation sector, advancing energy independence and reducing reliance on fossil fuels. Additionally, the process minimizes environmental pollutants, transforming them into valuable products like hydrogen and fuels, contributing to a cleaner and more sustainable future.

3. Table of Contents

4. Background:

Each year, the United States generates an estimated 77 million dry tons of sustainably collectable wet waste. But the significant water content of these wet wastes (typically >80%) becomes a bottleneck to recover the embedded energy using currently available technologies. Most of the wet waste is currently landfilled or anaerobically digested (AD) with biogas as a byproduct. However, landfilling occupies precious land without recovering values, while biogas generated via AD is of low-value and expensive to clean, leading to >80% of the biogas generated simply being flared off. Specifically, the U.S. discards ~15 million dry tons per year food waste with high organic content, but AD based systems are not very effective in converting food waste partially due to heterogeneity and high protein content. The state-of-the-art studies show that benchmark AD technology can convert food waste to raw biogas with a carbon efficiency at an average value of 41%. However, due to the large discrepancy in food waste composition, the actual carbon efficiency can vary significantly, from 29%-57%.

Compared to the raw biogas which has low economic value to potential greenhouse gas effects, our team from Princeton University, Pacific Northwest National Laboratory (PNNL), and University of Illinois at Urbana Champaign (UIUC) proposed to develop a synergistic approach to enable a total conversion of food waste to high quality renewable jet fuel blend stocks while also solving its aqueous phase problem (Figure 1). Hydrothermal liquefaction (HTL) can effectively convert high-protein wet waste to biocrude oil which can be further upgraded into transportation fuel. However, the wastewater generated during HTL has become a major bottleneck in its application. The

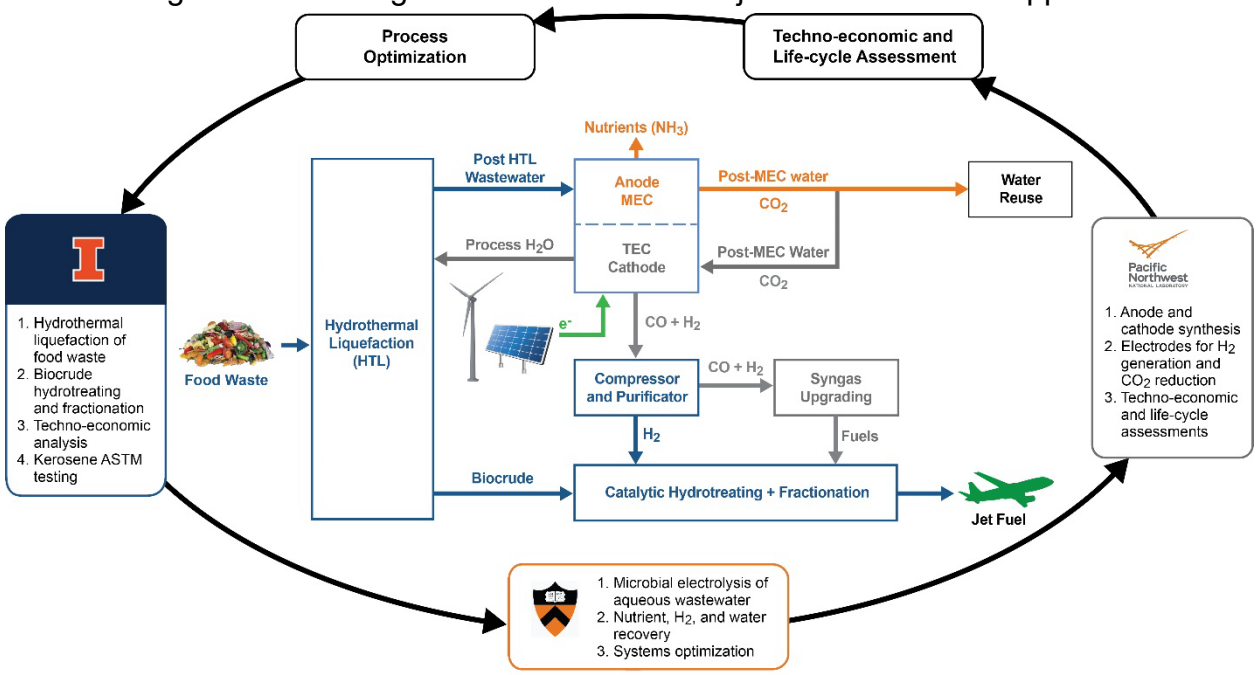

Fig. 1 The overall process and structure of the project. We developed a synergistic thermo-microbial-electrochemical (T-MEC) process that systematically increases the carbon efficiency and reduces costs by converting food waste to drop-in jet fuel blend stocks and simultaneously treating aqueous wastewater and recovering H_2 and nutrients. TEA and LCA were performed as system level analyses and optimization guidance.

post-HTL wastewater (PHW) is difficult to treat, and it reduces the process carbon efficiency by leaving a significant portion of carbon in the aqueous waste. On the other hand, upgrading HTL biocrude (including hydrotreating and hydrocracking process) requires a large amount of H_2 (currently generated via steam reforming of natural gas), which is a significant cost item. Valorization of PHW becomes a critical step towards the success of this waste-to-energy strategy. With the integration of the proposed synergistic Thermo-Microbial-Electrochemical (T-MEC) technology approach, the H_2 can be directly produced from PHW using biocatalysis-electrocatalysis reactors for biocrude upgrading, and the aqueous carbon/CO_2 can be recycled electrochemically back for closed-loop H_2 and biofuel conversion. Therefore, the overall carbon efficiency can be substantially improved, and waste disposal costs can be reduced from current practice.

5. Project Objectives:

The overall goal of this project is the successful development of a synergistic thermo-microbial-electrochemical (T-MEC) process that converts food waste to drop-in jet fuel blend stocks and simultaneously treats aqueous wastewater and recovers H_2 and nutrients. The T-MEC process targets to 1) improves the carbon yield by >50% compared to the anaerobic digestion baseline (35-45%) and 2) decrease the waste processing cost by >25% compared to AD.

Through this project, we will prove from prototype pilot scale reactors that T-MEC process can sustainably produce sufficient amount renewable jet blend stocks for testing using actual food waste, and the post-HTL wastewater (PHW) will be converted to additional fuel and energy. The reactors will be operated continuously for the long term under realistic conditions. We will gain key operating parameters to improve reactor performance and product quality, and we will perform TEA and LCA analyses to guide system development and technology commercialization.

In this project we will produce jet fuel blend from food waste using hydrothermal liquefaction (HTL) technology. The PHW will be valorized into H_2 and CO_2 using a microbial electrolysis (MEC) system. Using wastewater for H_2 generation instead of NG will increase the carbon yield of HTL, decrease the operation cost associated with NG consumption, and remove the H_2 generation plant. Upgrading the organics present in the PHW will lower the cost of waste disposal, and upgrading the CO_2 into biofuel will increase the carbon yield. To achieve this goal, we will start with lab scale validations to prove the feasibility of individual units, and we will develop novel catalysts and systems to improve conversion efficiencies. We will then collaborate to develop integrated pilot systems to convert food waste into jet fuel blends with PHW valorization and H_2 and NH_3 recovery. During the process, we will perform system-level analyses including TEA and LCA to identify the gaps and provide guidance on system development.

The budget periods and process targets included:

1. improve carbon yield by >50% compared to the anaerobic digestion baseline
2. decrease waste processing cost by >25% compared to baseline

Proposed Budget Period	Tasks	Go/No-Go Decision
01/2021-03/2021	Initial verification	All baseline data will be verified successfully
04/2021-03/2023	Reactor development, product upgrading, and material innovation	Carbon conversion efficiency improves by >25% from AD baseline and/or Disposal costs are reduced by > 15%
03/2023-12/2024	Pilot reactor development and operation, system analyses	Carbon conversion efficiency improves by >50% from AD baseline and/or Disposal costs are reduced by > 25%

The specific technical milestones proposed and accomplished include:

Project task descriptions and milestones	Date Completed
[Milestone 1.1] Initial benchmark verification on each process block	04/01/21
[Milestone 2.1] Food waste convert to biocrude oil and PHW	07/01/21
[Milestone 2.2] HTL biocrude characterization and distillation	07/01/21
[Milestone 2.3] Catalytic upgrading to bio-kerosene	07/01/23
[Milestone 2.4] Bio-kerosene quality assessment	04/01/24
[Milestone 3.1] Active gas harvesting module development	07/01/22
[Milestone 3.2] Catalysts and electrodes development and testing	10/01/22
[Milestone 3.3] Establishment of relationship between PHW composition and MEC performance.	07/01/23
[Milestone 3.4] Pilot MEC design, construction and start-up	10/01/23
[Milestone 4.1] Development of cathodic materials for H2 generation	04/01/23
[Milestone 4.2] Development of cathodic materials for syngas generation	10/01/23
[Milestone 4.3] Syngas utilization option analyses and demonstration	12/01/23
[Milestone 5.1] Integration and Testing of T-MEC Pilot System	01/01/24
[Milestone 6.1] Development of TEA and LCA models	04/01/24
[Milestone 6.2] Cost and carbon yield assessment and optimization	07/01/24
[Milestone 6.3] Refinement of TEA/LCA models	07/01/24

7. Project Results and Discussion:

The project results and discussion are organized based on the specific tasks that were led by different groups, and specifics are detailed in each task section.

Task 2: Converting food wastes into biocrude and upgrading into jet fuel blend using hydrothermal liquefaction (HTL) (Lead: UIUC Zhang Group)

2.1: Produce HTL biocrude oil and PHW using HTL pilot reactor

The hydrothermal liquefaction (HTL) of food waste was carried out in a pilot-scale continuous plug-flow reactor and results of the work were published[1]. Two types of food waste were collected in Champaign, IL: salad dressing waste (SDW) from a commercial food processing plant and Harvest Market food waste (HMFW) from a grocery store. The biochemical composition of each food waste is listed in **Table 2.1**. After collection, the feedstocks were homogenized with a food processor, pressed through a 16-mesh sieve, and diluted with water to the desired solids content to obtain a uniform slurry.

Table 2.1. Biochemical composition of the HTL food waste feedstocks (dry basis).

Characteristic	HMFW	SDW
Moisture (%)	66.73	75.66
Dry matter (%)	33.27	24.34
Protein (%)	32.76	2.38
Lipid (%)	29.10	62.45
Ash (%)	7.15	5.71
Carbohydrate[a] (%)	30.99	29.46
Carbon (%)	55.38	60.94
Hydrogen (%)	7.69	8.27
Nitrogen (%)	5.62	0.70
Oxygen[a] (%)	27.21	27.45
Sulfur (%)	0.33	<0.01
HHV (MJ/kg)[b]	25.74	28.04

[a]Calculated by difference
[b]Calculated by Dulong's formula

The pilot-scale HTL system (**Fig. 2.1**) consisted of a feedstock tank and pump, high-pressure pump, counterflow heat exchanger, PFR, rupture discs and pressure relief vessel, and back pressure regulators. The HTL reaction parameters in the published study were 280 °C, 11 MPa, 30 minute retention time, and 20 wt% total solids in the feedstock slurry. Before running feedstock through the reactor, the system was brought up to temperature in a heat-up phase using water. After maintaining reaction temperature for an hour, the feedstock slurry was added. 75 L of each feedstock was run consecutively, yielding about 150 L of HTL product (biocrude, PHW, and char). A primary vessel collected the HTL products, with a belt oil skimmer to separate oil after gravitational settling, and solids in each product stream were filtered out with a bag filter.

In additional runs, the HTL reaction parameters were 300 °C, 11 MPa, 20 minute retention time, and 20 wt% total solids content. The longest continuous run converted 300 L of SDW and 150 L of HMFW feedstock. At these conditions (300 °C, 20 min), the reactor feed rate was 90 kg/h, on track to process up to 2160 L of feedstock per day and yield about 200 L of biocrude per day, meeting Milestone 2.1. Furthermore, the conversion efficiencies for HTL biocrude oil are reported in **Table 2**. The biocrude oil yield from SDW exceeded the project's goal, while the carbon efficiency was just met.

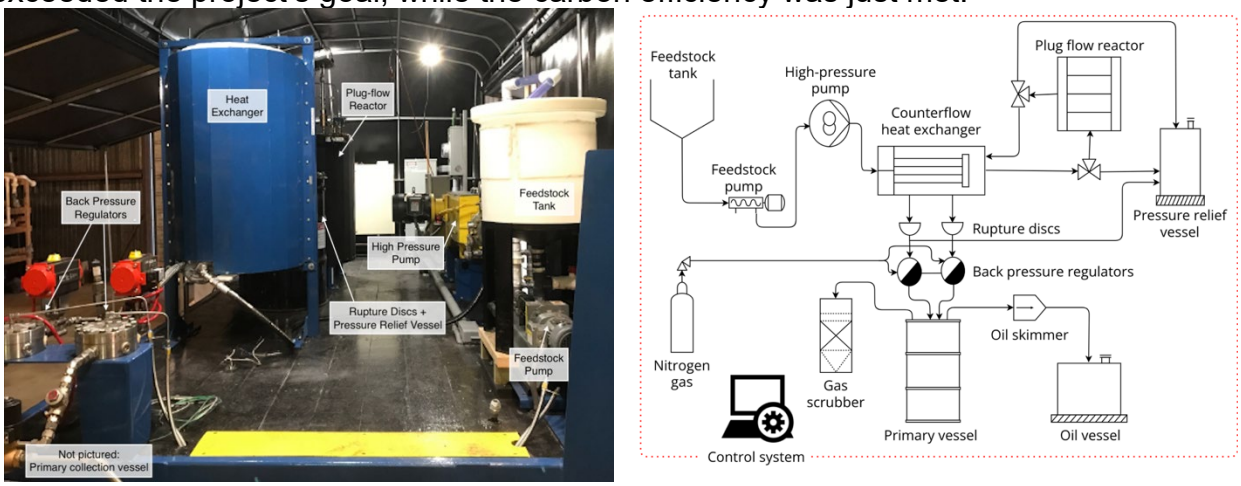

(a) (b)

Figure 2.1. Pilot-scale HTL reactor system (a) pictured and (b) process flow diagram.

Table 2.2. Mass yield and carbon efficiency of HTL biocrude oil (dry basis).

HTL Run	**Mass yield (wt%)**		**Carbon efficiency (%)**	
	SDW	HMFW	SDW	HMFW
2022	48.54	44.7	60.25	63.56
2023	59.35	41.28	69.32	60.76

Validation criteria	**Goal**	**Actual attained**
Mode of operation	Continuous	Continuous
Feed rate (kg/h wet feedstock)	90	90
HTL biocrude oil mass yield (DAF wt%)	50	59.3
HTL biocrude oil carbon efficiency (%)	70	69.3

2.2: Characterization and distillation of HTL biocrude oil into distillate fractions via physio-chemical processes

After recovery, HTL biocrude oil was dewatered according to ASTM D2892 Annex X1 to remove about 45 wt% of residual moisture. The characterization of dewatered HTL biocrude oil is listed in **Table 3**. It was seen that biocrude oil from both feedstocks still retained a significant amount of nitrogen, oxygen, and sulfur heteroatoms. Despite this, both HTL biocrude oils had high hydrocarbon content and higher heating value (HHV), making them suitable precursors for upgrading to biokerosene.

Table 2.3. Physicochemical properties of HTL biocrude oil

Property	GFW			SDW		
Carbon (%)	78.74	±	0.11	75.64	±	0.02
Hydrogen (%)	11.31	±	0.02	11.42	±	0.25
Nitrogen (%)	3.36	±	0.01	0.76	±	0.07
Oxygen (%)	6.46	±	0.14	12.16	±	0.30
S (%)	0.12			0.01		
H/C (mol:mol)	1.72	±	0.00	1.81	±	0.04
N/C x10 (mol:mol)	0.36	±	0.00	0.09	±	0.01
O/C (mol:mol)	0.06	±	0.00	0.12	±	0.00
HHV (MJ/kg)	40.32	±	0.07	38.57	±	0.32
TAN (mg KOH/g)	140.66	±	4.20	132.04	±	8.54
Density (g/mL)	0.95	±	0.00	0.93	±	0.00

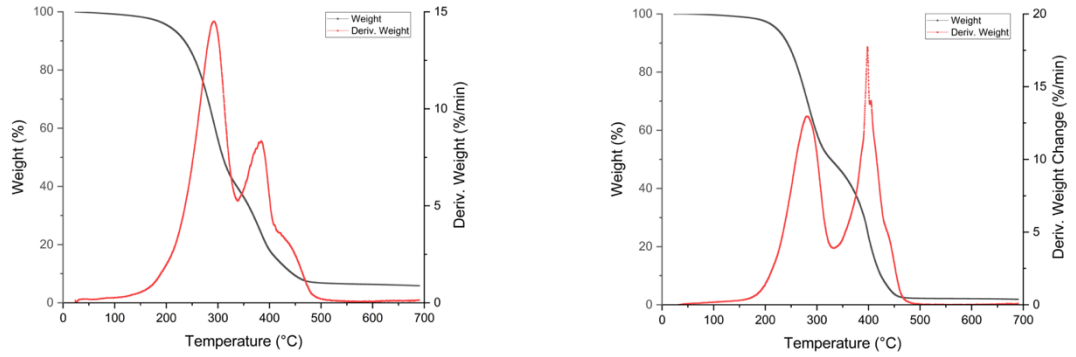

(a) (b)

Figure 2.2. Thermogravimetric analysis of HTL biocrude oil from a) HMFW and b) SDW.

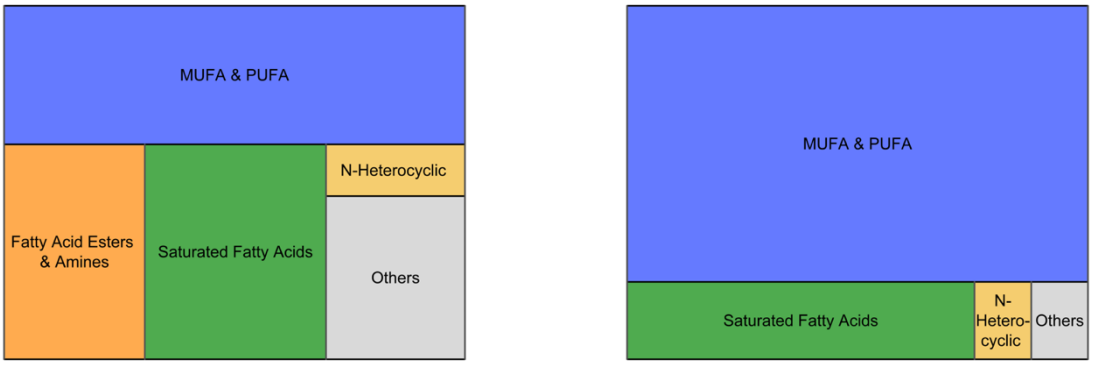

(a) (b)

Figure 2.3. Relative peak area of chemical compounds detected with GC-MS for HTL biocrude oil from a) GFW and b) SDW.

Gas chromatography mass spectrometry (GC-MS) showed that the biocrude oil components (**Fig. 2.3**) were a mixture of long chain acids (monounsaturated fatty acids (MUFA), polyunsaturated fatty acids (PUFA), and saturated fatty acids), fatty acid esters and amine, N-heterocyclic compounds, and others. The highest concentration in biocrude oil from both feedstocks were long chain acids, likely formed during hydrolysis of triacylglycerides[2]. Compared to SDW, biocrude oil from GFW contained a significant

amount of fatty acid esters and amines, likely due to the recombination of lipids and amines from degraded protein in the feedstock.

After characterization of the initial HTL biocrude oil, SDW biocrude was pretreated to remove inorganic contaminants (salt, water, ash) and isolate the light fraction (150-350 °C) prior to upgrading. HTL biocrude with high inorganic content should be pretreated to remove salt, water, and ash prior to hydroprocessing to prevent catalyst deactivation, corrosion, and equipment fouling during downstream activities[3]. A set of desalting (DSW) experiments, was designed to identify the effects of water:oil (W:O) ratio, retention time (RT), and temperature on desalting efficiency. Biocrude oil and deionized water were mixed and heated to a set temperature. After removing the salt-containing aqueous phase, ash and other solid residue were removed from the biocrude oil in a deashing (DSWA) stage with short-path simple distillation under atmosphere[4].

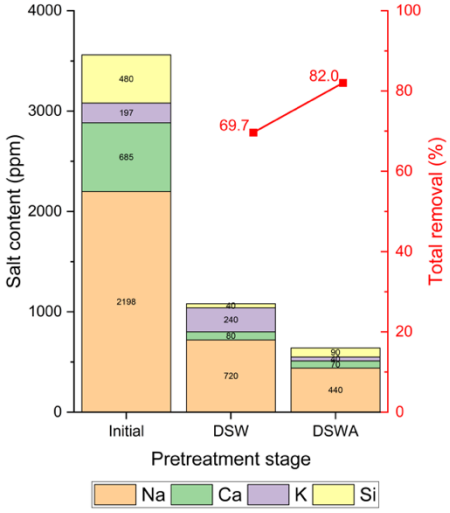

Figure 2.4. Concentration of salt in the FPW biocrude oil after each pretreatment stage

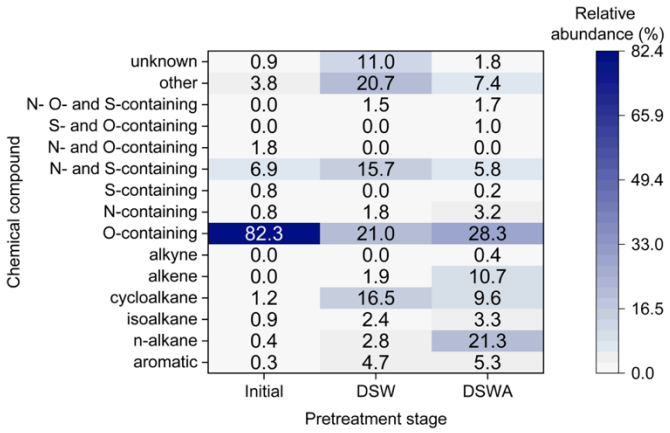

Figure 2.5. Chemical composition of the FPW biocrude oil before and after pretreatment stages

Total salt removal was maximized at 1:1 W:O ratio, 60 minute, and 100 °C, with a final salt content of 1,080 ppm. The salt content was further reduced after DWSA, with a total removal of 82.0% and final concentration of 640 ppm (**Fig. 2.4**). Additionally, GC-MS analysis shed light on changes in chemical composition of the biocrude oil during pretreatment (**Fig. 2.5**). It was observed that after pretreatment, oxygen-containing compounds decreased while hydrocarbon compounds increased. Distillation has been demonstrated to reduce heteroatoms leading to lower levels of oxygenated compounds, which could be due to decarboxylation and deamination reactions occurring at higher temperature[5]. The pretreated biocrude oil also had a much higher amount of hydrocarbons, with greater amounts of aromatics, n-alkanes, isoalkanes, cycloalkanes, and alkenes. These hydrocarbon compounds are ideal for hydrotreating, as the alkenes can undergo double bond saturation and long carbon chains can be hydrocracked or isomerized[6,7]. Similarly, the heteroatom-containing compounds can undergo hydrogenation to remove oxygen, nitrogen, and sulfur.

Physicochemical characterization (**Table 2.7**) and TGA (**Figure 2.6**) of HTL biocrude oil confirmed the improved fuel properties and isolation of the light fuel fraction. Overall, the physicochemical properties were improved, with a 5.3% increase in HHV, 23.5% decrease in TAN, 87.7% decrease in kinematic viscosity, and 7.2% decrease in density. These improvements were attributed to the removal of ash and heavy oil fraction after the DSWA stage, which helped isolate heteroatoms contained in the heavier fractions and provide a more stable biocrude oil composition[5]. The shift in boiling point distribution to the left reflects the removal of higher boiling point compounds from the biocrude oil. Furthermore, the minor weightloss peak at was nearly eliminated, with just the major weightloss peak at 300 °C remaining. The decrease in the heavy fraction also explains the decreased density of the pretreated biocrude oil.

Table 2.7. Physicochemical properties of initial and pretreated FPW biocrude oil

	Initial			**DSW**			**DSWA**		
Carbon (wt%)	75.57	±	0.23	75.44	±	0.07	77.97	±	0.11
Hydrogen (wt%)	11.31	±	0.03	11.25	±	0.06	12.02	±	0.02
Nitrogen (wt%)	0.64	±	0.02	1.03	±	0.04	0.72	±	0.02
Oxygen (wt%)	12.45	±	0.23	12.26	±	0.17	9.28	±	0.11
Sulfur (wt%)	0.040			0.035			0.018		
HHV (MJ/kg)	38.37	±	0.14	38.30	±	0.12	40.39	±	0.03
TAN (mg/g)	185.17	±	5.92	223.26	±	2.44	141.60	±	2.18
Viscosity (mm^2/s)	119.87	±	2.01	86.53	±	2.55	14.79	±	0.13
Density (g/mL)	0.926	±	0.00	0.912	±	0.001	0.859	±	0.001

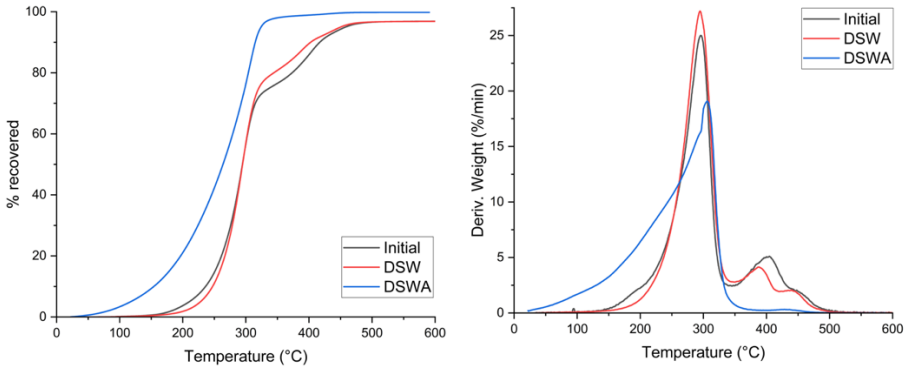

Figure 2.6. a) TGA and b) DTG peaks of the initial and pretreated FPW biocrude oil.

HTL biocrude oil was pretreated to remove inorganic content (i.e. water, salt, ash) in preparation for catalytic upgrading. The effect of desalting parameters, along with physicochemical characterization and TGA demonstrated the properties of the isolated fuel fraction from HTL biocrude oil. Notable achievements were that water and ash were completely removed, and the salt content of the HTL biocrude oil was reduced from 3,560 to 640 ppm, meeting the recommendation from PNNL for salt level <1,000 ppm prior to upgrading.

2.3: Catalytic upgrading of distillate fractions to achieve bio-kerosene production

Commercial catalyst $CoMo/Al_2O_3$ (ThermoFisher Scientific) was used to hydrotreat HTL biocrude oil. First, a Taguchi design L9 orthogonal array was used to screen the significance of temperature (T), catalyst-to-oil ratio (cat:oil w/w), retention time (RT), and hydrogen load-to-biocrude oxygen ratio (H:O mol:mol). Then, a Box-Behnken design was used to optimize the parameter levels using response surface methodology, where T was 350-450 °C, cat:oil was 0.1-0.5 w/w, and RT was 2-4 h.

The parameter screening tests revealed that T > cat:oil > RT had the greatest effect on deoxygenation, carbon recovery, and energy recovery. Parameter optimization showed that temperature had the greatest effect on the average carbon number and carbon range distribution of the upgraded HTL biocrude oil. Average carbon number and hydrocarbon type are significant properties in predicting the properties of SAF[8,9]. Heat maps elucidated the effect of T, RT, and cat:oil on the average carbon number of hydrotreated biocrude oil (**Fig. 2.7**). It was seen that T had a greater effect than RT on average carbon number, with decreases in carbon number correlated with increased T. The tilt of the contour lines toward the left also reflected decreased carbon number at longer RT, indicating breakdown of the carbon chains with limited repolymerization. Similar trends were seen for T and cat:oil, with decreased carbon number with increased T at all levels of cat:oil. Meanwhile, the change in carbon number across RT and cat:oil varied across levels. Overall, at combinations of higher levels of T, RT, and cat:oil, the average carbon number further decreased. Therefore, while a higher temperature was required during hydrotreating to achieve a decreased average carbon number that is closer to jet fuel, it should only be combined with moderate levels of RT and cat:oil to avoid SAF products with carbon chains that are too light.

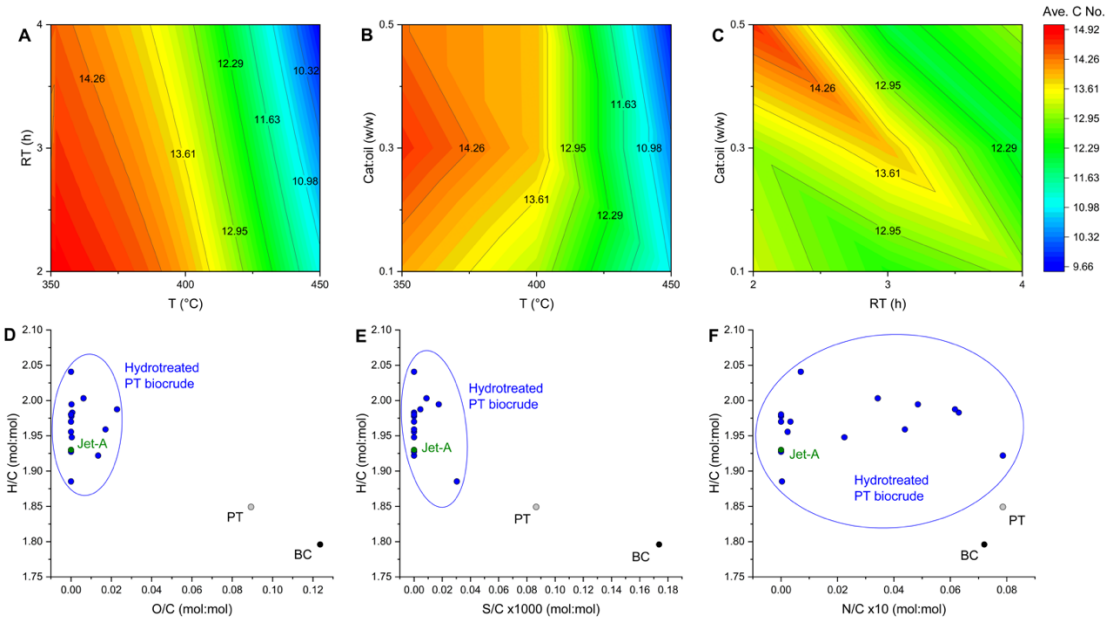

Figure 2.7. Average carbon number of hydrotreated HTL biocrude for A) retention time vs. temperature; B) catalyst ratio vs. temperature; C) catalyst ratio vs. retention time; and modified Van Krevelen diagrams comparing D) oxygen content; E) sulfur

content; F) nitrogen content of hydrotreated PT biocrude to the pretreated HTL biocrude (PT) and initial HTL biocrude (BC).

The modified Van Krevelen diagrams exhibit effective deoxygenation and desulfurization during hydrotreating, but varying denitrogenation (**Fig. 2.7**). A majority of the upgraded HTL biocrude underwent complete oxygen and sulfur removal. The Jet-A sample had an H/C ratio of 1.93. A majority of the upgraded HTL biocrude had H/C >1.90, reflecting their comparable elemental composition to Jet-A, high HHV, and potential for improved combustion. A wide range of de-nitrogenation was observed, with near and complete denitrogenation in a few cases. Considering the low nitrogen content in the initial HTL biocrude oil, the variation may also be due to systematic errors.

Comparing the hydrocarbon type, carbon number distribution, and boiling point distribution of the HTL biocrude oil before and after hydrotreating, it was confirmed that hydrotreating at high temperature produced SAF samples with composition closest to Jet-A (**Fig. 2.8**). Hydrotreating at combinations of higher temperature, retention time, and catalyst load improved the hydrocarbon type to contain increased amounts of aromatics, isoalkanes, and cycloalkanes. Compared to Jet-A, several upgraded biocrudes contained similar or higher amounts of iso- and cyclo-alkanes, along with lower aromatic content, which could lead to better cold flow properties and less contrails[10].

HTL biocrude oil composition became increasingly lighter after hydrotreating. This was reflected in the boiling point distribution, where hydrotreating increased the fraction of distillate ranges <230 °C (**Fig. 2.8B**). Hydrotreating at the lowest parameter levels caused polymerization reactions that formed heavier compounds with boiling points above 350 °C. On the other hand, all samples hydrotreated at the highest temperature level had a boiling point distribution more like Jet-A.

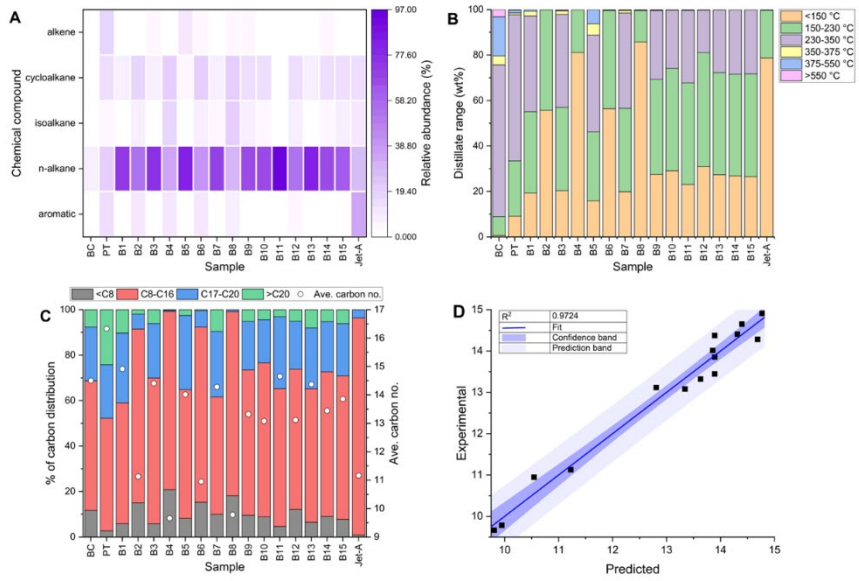

Figure 2.8. Fuel properties of the hydrotreated HTL biocrude oils, A) hydrocarbon composition; B) distillate ranges; C) carbon number distribution; and D) comparison of the predicted and experimental average carbon number from RSM correlation.

The carbon number range for Jet-A is typically C8-C16. This was confirmed in the commercial Jet-A sample tested, where 95% of its compounds were

within the C8-C16 range and its average carbon number was 11.2 (**Fig. 2.8C**). Chemical compounds were also grouped into carbon number ranges to represent potential distillates. All samples that had an average carbon number similar to or less than Jet-A (<11.5) were those produced at high temperature during hydrotreating (450 °C). Due to the importance of average carbon number on the chemical and handling properties of jet fuel, regression of the RSM data was used to predict the average carbon number and compare it to the experimental values (**Fig. 2.8D**). The predicted and experimental values were highly correlated, with R^2 = 0.97.

The final SAF sample was attained by hydroprocessing at 400 °C, 4h, and 0.5 cat:oil. Physicochemical properties of the upgraded HTL biocrude oil were listed in Table 8. The carbon and energy recovery was 85.2 and 90.2%, respectively. Complete deoxygenation and denitrogenation was achieved, along with a final sulfur content of 10 ppm, meeting the 15 ppm maximum.

Table 2.8. Physicochemical properties of the upgraded HTL biocrude oil

Property	**Value**
Carbon (wt%)	85.65 ± 0.08
Hydrogen (wt%)	14.53 ± 0.08
Nitrogen (wt%)	0.00 ± 0.00
Oxygen (wt%)	0.00 ± 0.00
Sulfur (ppm)	10
HHV (MJ/kg)	47.00 ± 0.13
Carbon recovery (%)	85.16 ± 0.08
Energy recovery (%)	90.20 ± 0.24
Total acid number (mg KOH/g oil)	0.96

Based on PNNL recommendation, $CoMo/Al_2O_3$ catalyst was used to achieve HDO conversion of HTL biocrude oil. Using this catalyst, 100% HDO was achieved. A continuous >100 h run was not completed due to the batch configuration of the reactor. However, enough HTL biocrude oil was upgraded to meet the volume requirements for the preliminary ASTM specification screening.

Validation criteria	**Goal**	**Actual attained**
Mode of operation	Continuous	Batch
Feed rate/scale	10 kg/h	100 ml
Upgraded fuel carbon efficiency (%)	80	85.2
HDO conversion (%)	>80	100

2.4: Assessment of the upgraded HTL kerosene with standard

The jet fuel cut (150-250 °C) of hydrotreated HTL biocrude oil from this work was characterized using Tier α tests at Washington State University (WSU) to prescreen its viability as a sustainable aviation fuel (SAF) by comparing its compositional, distillation, and fuel properties to conventional jet fuel and ASTM D4054 specifications[8,9].

Compared to conventional jet fuel, the SAF candidate from this work contained higher amounts of light hydrocarbons but was within ASTM specification limits for critical bulk properties (**Fig. 2.9**). The hydrocarbon compositions of both upgraded HTL biocrude oil and SAF cut were mainly n-alkanes, then cycloalkanes, aromatics, and isoalkanes. Compared to the average jet fuel carbon distribution, the hydrotreated HTL biocrude oil contained high amounts of lighter (<C9) and heavier (>C13) hydrocarbons. However, after taking the SAF cut from C9-C13, the average carbon number decreased to be more like jet fuel. This SAF cut represented 31.5% yield of the hydrotreated HTL biocrude oil; meanwhile, the light and heavy ends are also potential candidates for biobased gasoline and diesel fuel.

It was observed that the surface tension (σ), density (ρ), kinematic viscosity (v), lower heating value (LHV), flash point, derived cetane number (DCN), and freeze point were all within ASTM specification limits. Notably, the density and freeze point of the SAF candidate were near, but still, within ASTM specification limits, which was attributed to the high amount of heavy-end n-alkanes. On the other hand, lower heating value (LHV) was even higher than conventional jet fuel, likely due to the increased amount of n-alkanes. Since the SAF cut contained >50% n-alkanes, the fuel likely has a high smoke point, preventing soot formation and allowing for cleaner combustion. Meanwhile, the high amount of cycloalkanes and aromatics (~44%) also help to improve performance and handling properties of the SAF. Although the light and heavy ends fell slightly below the distillation curve for jet range, it was still within ASTM specification limits. Based on the predicted properties of the SAF cut, little to no blending may be required and hydrotreated HTL biocrude oil from food waste is a promising candidate for drop-in SAF.

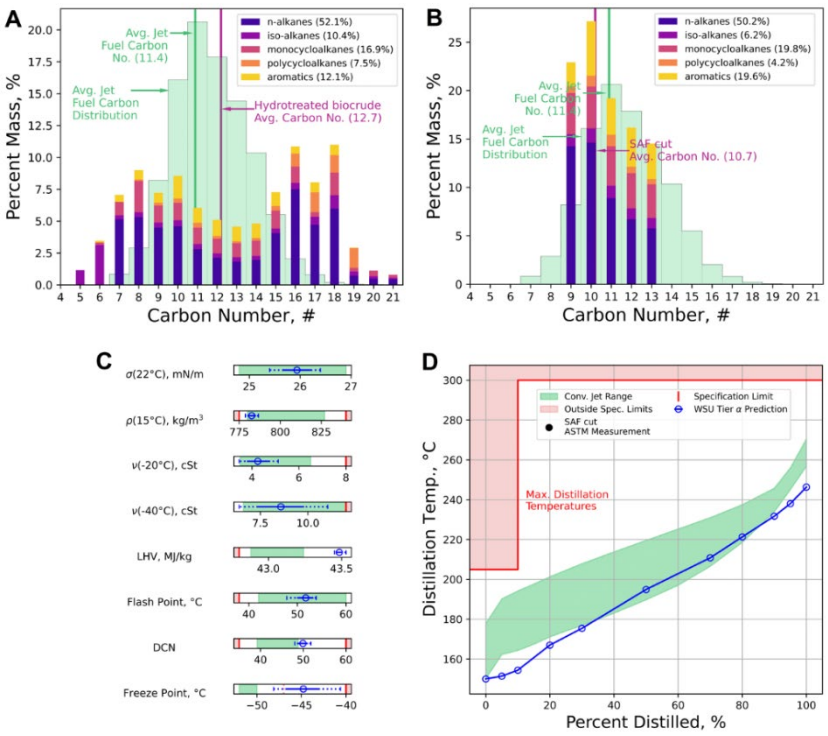

Figure 2.9. Tier α results for SAF candidate testing compared to conventional jet fuel including hydrocarbon type distribution of A) whole hydrotreated HTL biocrude oil and B) SAF cut from hydrotreated HTL biocrude oil; C) predicted jet fuel properties; and D) ASTM D86 distillation curve.

Bio-kerosene samples upgraded via hydrotreating HTL biocrude oil were sent to WSU for preliminary screening of SAF properties. It was found that the upgraded HTL biocrude oil met all critical ASTM specifications and its distillation properties were similar to conventional jet fuel.

Task 3: PHW treatment and conversion to H2 in MECs (Lead; Princeton Ren Group)

Microbial electrolysis cell (MEC) leverages the embedded chemical energy in high-strength wastewater for clean H_2 production, which can be utilized for biocrude upgrading to jet fuel. In this task, we developed MEC running on PHW as substrate that produces clean H_2 with low energy consumption 16-26 kWh/kg-H_2. We utilized analytical chemistry to elucidate the relationship between PHW composition and MEC performance. We found that volatile fatty acids and monohydric and polyhydric alcohols were effectively transformed through the synergistic metabolism of fermentative and electroactive bacteria, which led to over 70% chemical oxygen demand removal of the recalcitrant compounds and a record high H_2 production rate (1.62 L/L/d). We also employed the liquid-state ^{15}N nuclear magnetic resonance on wastewater samples for the first time and revealed that the nitrogen-containing heteroaromatics were persistent to microbial electrochemical treatment.

3.1. Lab-scale validation on PHW treatment with MEC

We first validated the PHW degradation results with lab-scale MEC. The wastewater contained highly concentrated organics, and the COD value was 57,500 ± 200 mg L^{-1}, approximately two orders of magnitude higher than domestic wastewater. The DOC content of the PHW was 17,853 ± 287 mg L^{-1}. The COD and DOC value combined will give an average degree of reduction of carbon of 4.8, marking the average carbon in PHW is slightly more reduced than biomass. The water was slightly alkalic with a pH of 7.97, and the conductivity was 18.4 mS cm^{-1}, indicating high ionic strength. Both inorganic salts and ionizable organic compounds such as VFAs contribute to the conductivity. The total inorganic concentration of the PHW was 404 ± 12 mg /L^{-1}, which includes carbonate (CO_3^{2-}), bicarbonate (HCO_3^-) and dissolved CO_2. The high conductivity and high alkalinity are beneficial to MEC treatment, as they facilitate electron transfer and provide high buffering capacity to alleviate pH gradient between electrode chambers. Based on the characteristics of the PHW, we carried out matrix experiments using different dilution ratios and applied voltages to identify the optimal operating conditions for the treatment of PHW and generation of H_2 from MEC reactors. Since the organic concentration is much higher than typical wastewater, we employed a range of dilution ratio from 40× (1.5 g L^{-1} COD) to 10× (6 g L^{-1} COD).

Results show that COD removal peaked at a dilution ratio of 20× (3 g L^{-1} COD), with a removal rate of 65% after one day under an applied voltage of 1.0 V (**Fig. 3.1B**). Kinetically, higher organic concentration leads to faster electron transfer toward the cathode, which consequently improves H_2 production rate (**Fig. 3.1C**). However, the total amount of organic to be removed also increased, which result in a lower removal efficiency for 10× dilution group. The highest H_2 production rate achieved was 1.62 L L^{-1}

day^{-1}, under an applied voltage of 1.0 V with 10× dilution, which successfully met the milestone. This value is one order of magnitude higher than the previous achieved rate (0.17 L L^{-1} day^{-1}) using swine manure PHW as feedstock under an applied voltage of 1.2 V. The COD to H_2 yield also shows a significant improve, with 0.074 kg-H_2 kg-COD^{-1} under this condition, compared to 1.028×10^{-5} kg-H_2 kg-COD^{-1} in the previous study. The high H_2 production rate reported here could be attributed to a robust electroactive community on the bioanode, whereas the high COD to H_2 yield indicates a relatively high contribution of electroactive bacteria to COD removal compared to non-electroactive species. The microbial characterization results will be discussed later.

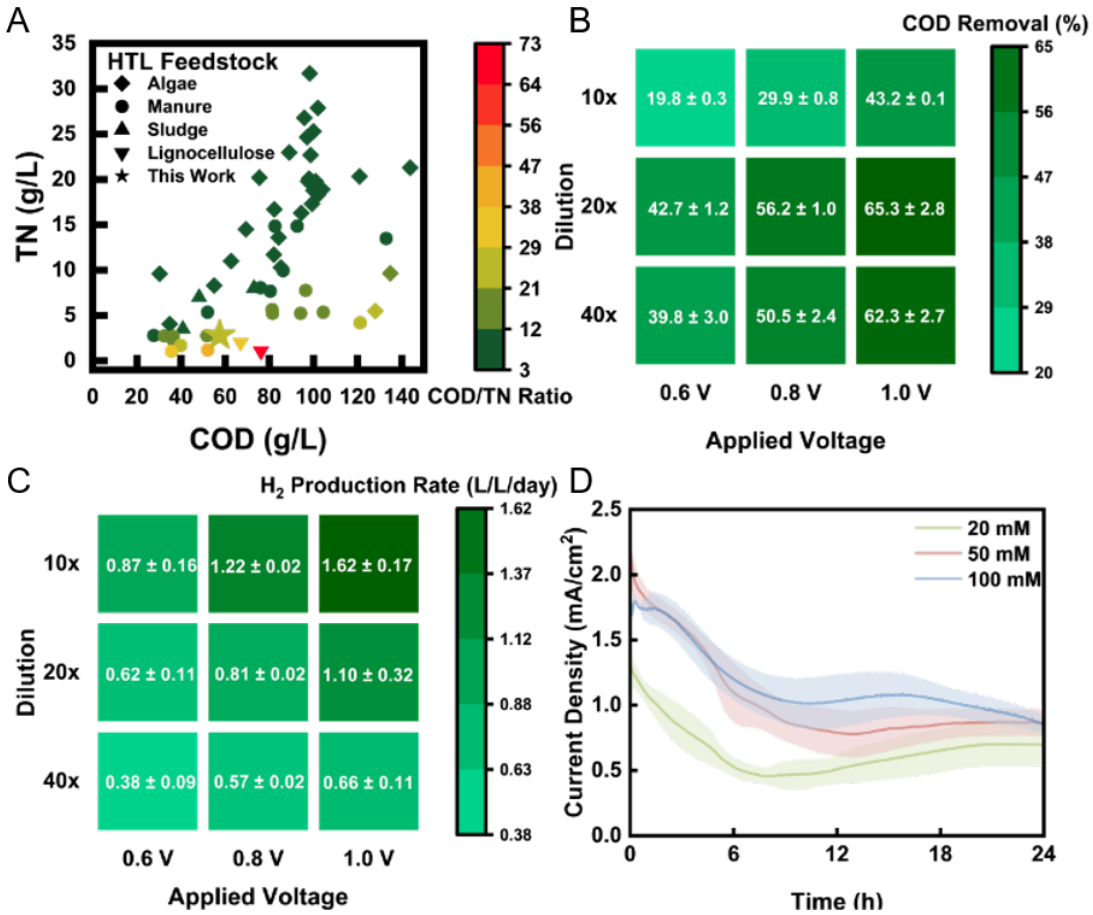

Figure 3.1. (A) COD/TN composition of feedstock PHW used in this study and other PHW studies; The COD removal (B) and H_2 production rate (C) of PHW-fed MEC in 3-day period under different applied voltage and dilution ratio. (D) The current density profile under different buffer strength after introduction of fresh electrolyte. The shadows represent standard deviation from triplicate experiments.

With the optimal parameters identified above (20x dilution, 1 V applied voltage, 100 mM PBS), we carried out MEC treatment of PHW and tracked the concentration of organic compounds throughout the experimental period[12]. As shown in **Figure 3.2 A&B**, the two major components – glycerol and acetate, were both quickly depleted after two days, but other compounds such ethanol and propionate showed different patterns. The fast

depletion of acetate is in line with previous findings, as acetate is a known favorable substrate for electroactive microbes. Many studies have shown that acetate led to the highest electron transfer efficiency by the common electroactive *Geobacter* spp. compared to other organics such as lactate and formate.

Different from acetate, glycerol cannot be directly metabolized by electroactive microbes, but its quick degradation was believed to be due to anaerobic fermentation. This is supported by the increase in concentration of 1,3-PDO, which is a common fermentation product of glycerol (**Fig. 3.2C**). In this pathway, glycerol is first dehydrated to 3-hydroxypropanal with glycerol dehydratase, which is then consequently reduced to 1,3-PDO through 1,3-PDO dehydrogenase. **Fig. 3.2A** shows 1,3-PDO concentration peaked after two days of PHW treatment, coordinated with glycerol depletion. 1,3-PDO concentration started to decrease after that, presumably due to consumption. Previously, sulfate-reducing bacteria strains isolated from freshwater sediments have been proven capable of using 1,3-PDO as substrate and converting it to acetate and CO_2 while reducing sulfate to sulfide.

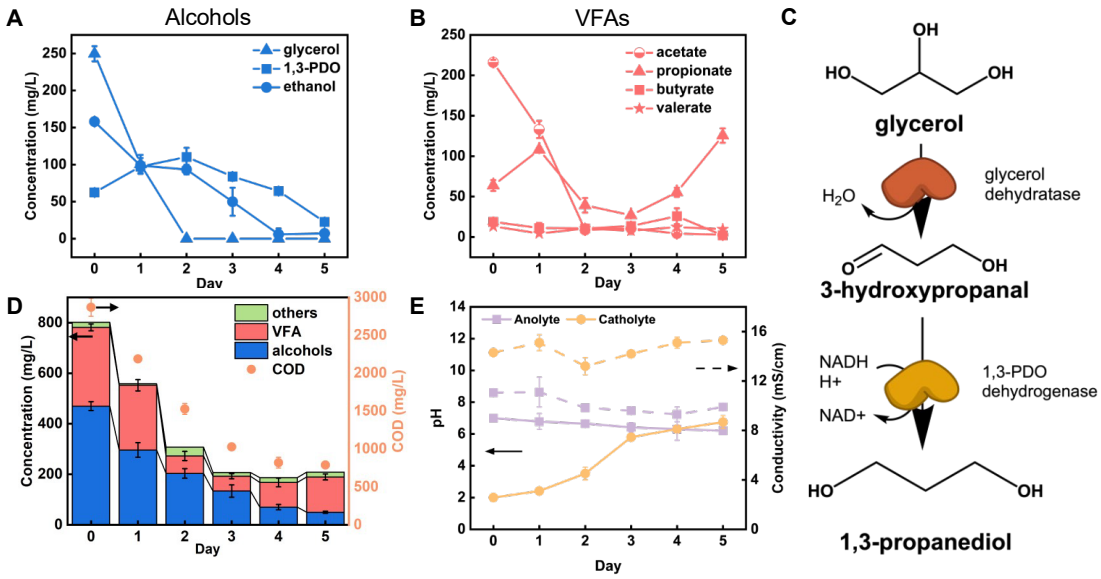

Figure 3.2. The concentration profile of (A) alcohols and (B) VFAs throughout the MEC treatment as identified by HPLC with an ion-exclusion column. (C) The metabolic pathway of glycerol fermentation to 1,3-PDO. (D) The combined concentration profile of HPLC identified chemicals and the COD degradation profile. (E) The pH and conductivity change of electrolyte throughout the MEC treatment. pH is presented by solid lines and conductivity by dashed line.

3.2. Establishing a metabolic network

A compact layer of biofilm was observed on the anode carbon fibers after MEC operation (**Fig. 3.3A**). To characterize the microbial communities and understand their functions in terms of organic and nitrogen transformation in the MEC, we collected initial biofilm samples right after inoculation and at the end of the experimental period. It was found that *Geobacter* spp. accounts for 70% abundance in both samples, indicating robust

electroactive activities (**Fig. 3.3B**). The dominantly high abundance of *Geobacter* spp. could be originated from the relatively low anode potential (-0.35 V vs Ag/AgCl) during inoculation, which has been shown to select for electroactive bacteria conducting direct extracellular electron transfer. The most notable difference in biofilm ecology after PHW treatment is the increase in sulfate-reducing bacteria - *Desulfovibrio* spp., from 0.2% to 7.5%. The increase could be attributed to the presence of 1,3-PDO in PHW, which *Desulfovibrio* spp. have been shown to degrade with sulfate as the terminal electron acceptor. The *Anaerotignum* spp. could be responsible for propionate production during MEC treatment, as *Anaerotignum propionicum* (formerly known as *Clostridium propionicum*) has been demonstrated to ferment glycerol to propionate with a yield of 79.6%. The other major genera - *Acetobacterium* and *Lactococcus*, are all anaerobes which conduct either fermentation or anaerobic respiration. The presence of methanogens, including *Methanobrevibacter* and *Methanomassiliicoccus*, indicate possible CO_2 recycling where the CO_2 produced from COD oxidation were subsequently converted to methane.[12]

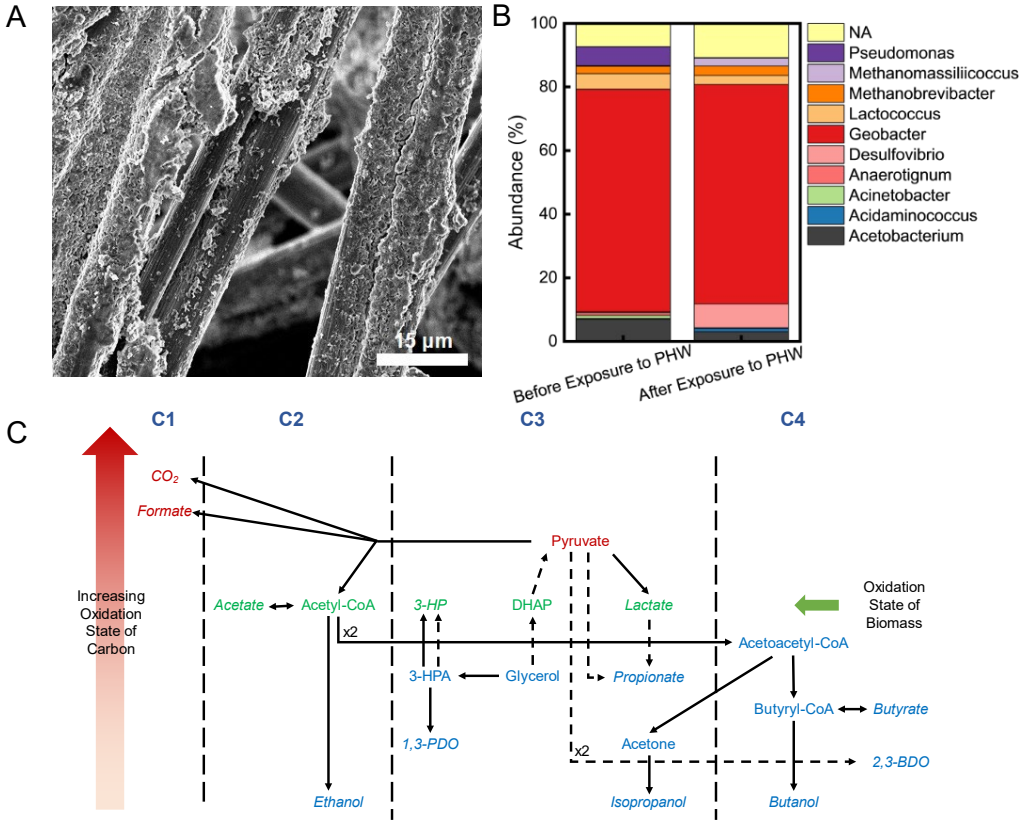

Figure 3.3. (A) SEM image of the layer of biofilm formed on carbon fibers. (B) Genus-level biofilm composition before and after exposure to PHW. (C) The proposed metabolic network in the anode chamber. Dashed arrows represent multiple-step processes. The metabolites are arranged in ascending order of carbon valency from bottom to top, and in increasing order of the number of carbon atoms from left to right. Metabolites written in italic represent possible direct electron donors for electroactive bacteria. The color of the metabolites suggests the average degree of reduction of the carbon, with blue indicating

more reduced than biomass, green indicating the same degree of reduction as biomass, and red indicating more oxidized than biomass.

The fermentative bacteria together account for < 30% abundance on the anode biofilm, yet they played an important role in COD degradation. The raw PHW contains a high concentration of glycerol (4,992 ± 253 mg L^{-1}) that is not readily available for electroactive bacteria. Glycerol is therefore first fermented through various pathways to fermentation end products such as 1,3-PDO, ethanol, acetate, and propionate, as shown in HPLC analysis, which were then subsequently available as electron donor to electroactive bacteria such as *Geobacter* spp. (**Fig. 3.3C**).

Task 4: Lab-scale study on PHW to H_2 in TEC (PNNL, Lead: Lopez-Ruiz Group).

In this task, the PNNL team developed cathodic materials for the electrocatalytic generation of H_2 in PHW. They worked with the Princeton team (Task 3) to test these electrodes in the MEC and collaborated with the Analysis team (Task 6) to identify best gas management strategies (H_2) as well as evaluate costs of the different electrolyzers.

4.1.TEC cathode performance using different metals

We explored the electrochemical performance of different BGM- and PGM-based electrodes with equimolar metal loadings using a 5X diluted real food wasted-derived PHW buffered with the same formulation used in the MEC, 0.10 M NaH_2PO_4/Na_2HPO_4. As shown in **Figure 4.1**, all the TEC cathodes were able to meet the milestone when operating at 27 A/m^2 (2.7 mA/cm^2) TEC system in real food waste-derived HTL-derived generated at PNNL (with COD = 85,000 ppm) under a broad range of electrochemical reaction conditions. The electrodes containing BGM (e.g., Ni, Cu, and Co) performed similarly to those with PGM (Pt, Ru, and Pd). Because of the 2 to 3 times higher molecular weight of the PGM compared to the BGM, the BGM resulted in an overall higher specific H_2 production rate [i.e., mmol $H_2/(g_{metal} \cdot h)$]. However, all the catalysts were capable to surpass the milestone of 100 mmol $H_2/(g_{metal} \cdot h)$ using PHW when operating at current densities > 27 A/m^2.

Figure 4.1 b and c shows that the energy efficiency and consumption for H_2 generation (kWh/kgH_2) was similar for all the PGM and BGM tested within a factor of 2; however, an unexpected trend was observed as the PGM (Ru and Pd) were slightly more active than the BGM at current densities <55 A/m^2 but the BGM (Ni and Cu) were more active than the PGM at current densities >110 A/m^2. These results suggests that expensive PGMs are indeed not needed for H_2 generation for the low currents at which the PHW electrolyzers operate. Because BGM had similar H_2 generation performance than PGM but had lower molecular weight, the specific H_2 production of the BGM are between 2 and 5 times lower than PGMs (**Figure 4.1d**).

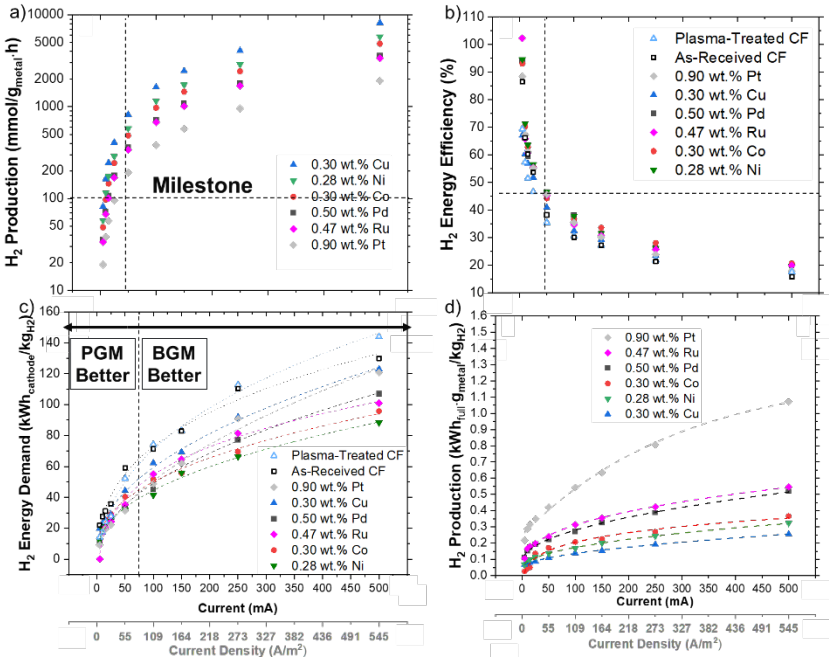

Figure 4.1. Performance for TEC system for H_2 production using real food waste-derived 5X diluted PHW with 0.1 M NaH_2PO_4/Na_2HPO_4 as a function of current and electrode (cathode) composition. The anode was a PNNL proprietary material. All the cathodes were synthesized with equimolar metal loading, the difference on final metal weight loading content was caused by the changes in molecular weight. The results were obtained in single-pass configuration using flow rates of 4 to 10 scm^3/min.

4.2. TEC performance under different dilution ratios, buffers, and applied voltages

We explored the electrochemical performance of the TEC system in real food waste-derived HTL-derived generated at PNNL (with COD = 85,000 ppm) under a broad range of electrochemical reaction conditions. The PHW was filtered and evaluated with and without buffers and with and without 5X diluted conditions. As shown in **Figure 4.2**, the TEC system was able to produce H_2 at 4,000 mmol $H_2/(g_{metal}·h)$ (at >5 V) regardless of the electrolyte compositions and exceed the H2 production milestone of 100 mmol $H_2/(g_{metal}·h)$. However, the energy required to produce H_2 changed depending on the current (density) as well as the electrolyte composition. As shown in Figure Xa and b, the TEC system performed similarly regardless of the buffer agent used at low current, >5 mA or 5.6 A/m^2); however, upon increasing the current to 500 mA (545 A/m^2), the energy requirements to produce the H_2 (kWh/kgH_2) was clearly affected by the presence of the (0.5 M) buffer. Overall, a ≈40% decrease in energy consumption was observed when using buffers as opposed to no-buffer. The energy consumption trend goes as follows: KOH < NaH_2PO_4/Na_2HPO_4 < Na_2SO_4 < No buffer. Upon dilution of wastewater by 5X (**Figure 4.2b**), we observed that the buffered wastewaters behaved similarly; however, the energy consumption was slightly higher than under the undiluted systems. We speculate that the differences in pH as well as the concentration of the buffer salts are responsible for the small changes in performance.

Regardless of the buffer and dilution, the TEC system was operating at >50% energy efficiency for H_2 generation (defined as H_2 high heating value divided by electrical power used in the TEC system) at current densities <25 A/m^2, showing >100% energy when operating at <6 A/m^2. Increasing the current density to up to 545 A/m^2 causes the energy efficiency to decrease to as low as 20%, due to the increase in the cell voltage required to produce the high current density.

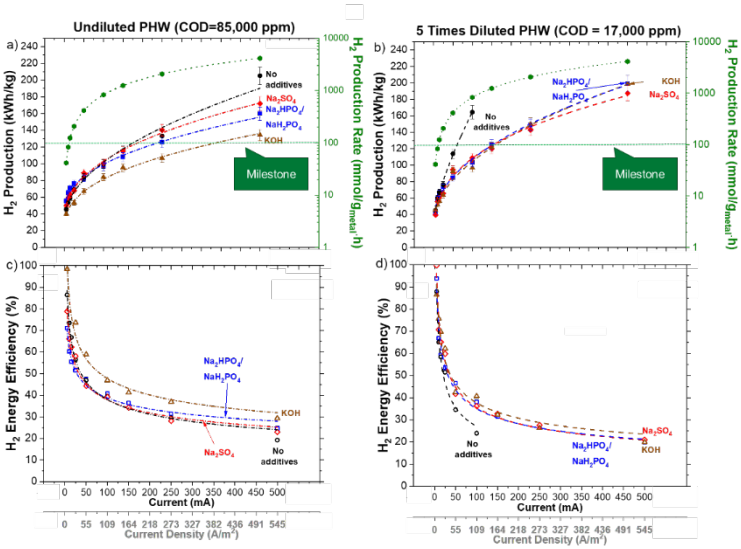

Figure 4.2. Performance for TEC system for H_2 production using real food waste-derived PHW as a function of current in the presence of additives and dilutions. The anode was a PNNL proprietary material. The cathode was a 0.5 wt.% Pd supported on a carbon felt (0.5 wt.% Pd/CF). The concentrations of salts and buffers was constant at 0.5 M for the undiluted system and 0.1 M for the diluted system. The results were obtained in single-pass configuration using flow rates of 4 to 10 scm^3/min.

4.3.TEC long term stability performance

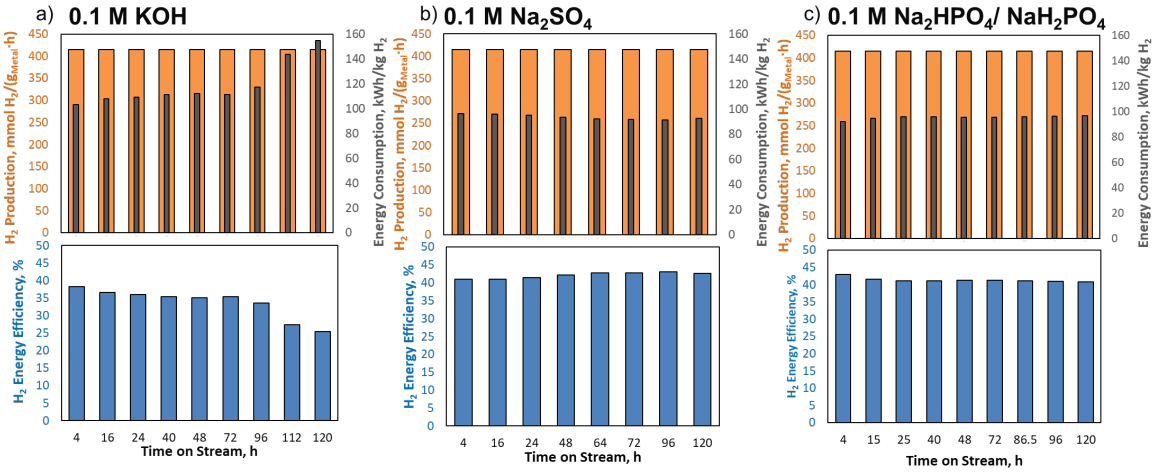

Figure 4.3. Long term stability performance of the TEC system for treatment of 5X diluted food waste-derived PHW when using different additives such as a) 0.1 M KOH, b) 0.1 M Na_2SO_4, and c) 0.1 M Na_2HPO_4/ NaH_2PO_4). The anode was a PNNL proprietary material. The cathode was a 0.5 wt.% Pd supported on a carbon felt (0.5wt.% Pd/CF). The experiments were run at constant current density of 55 A/m^2 and full recycle of 150 mL constant volume of solution recirculating thought the cell at 4 scm^3/min.

We assessed the TEC and electrode's long-term stability using 5X diluted real food waste-derived PHW under a constant current density of 55 A/m^2. As shown in **Figure 4.3**, the system operated at near 400 mmol H_2/(g_{metal}·h) for 120 h/test (>360 h total), meeting the milestones for H_2 production and stable run of >100 mmol H_2/(g_{metal}·h) and >100 h, respectively. Only when operating with without KOH, we observed a change in the power consumption after 72 h of operations associated with changes in solution pH. However, this was not an issue when operating with 0.1 M of Na_2HPO_4/ NaH_2PO_4 or Na_2SO_4 buffered solutions as the performance was constant for 120 h. The constant energy efficiency and energy consumptions is caused by stable operation potentials, which

indicates that the electrodes do not degrade under reaction conditions. **Figure 4.4** shows the change in coloration of the diluted sample solutions as a function of time of stream.

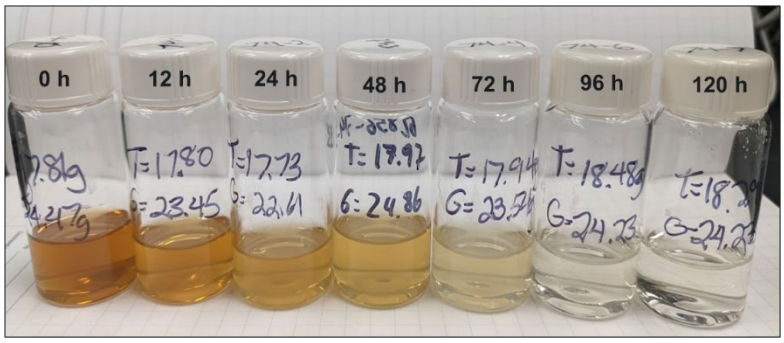

Figure 4.4. Change in coloration of diluted PHW sample as a function of time on stream when operating at 55 A/m^2 and full recycle operation.

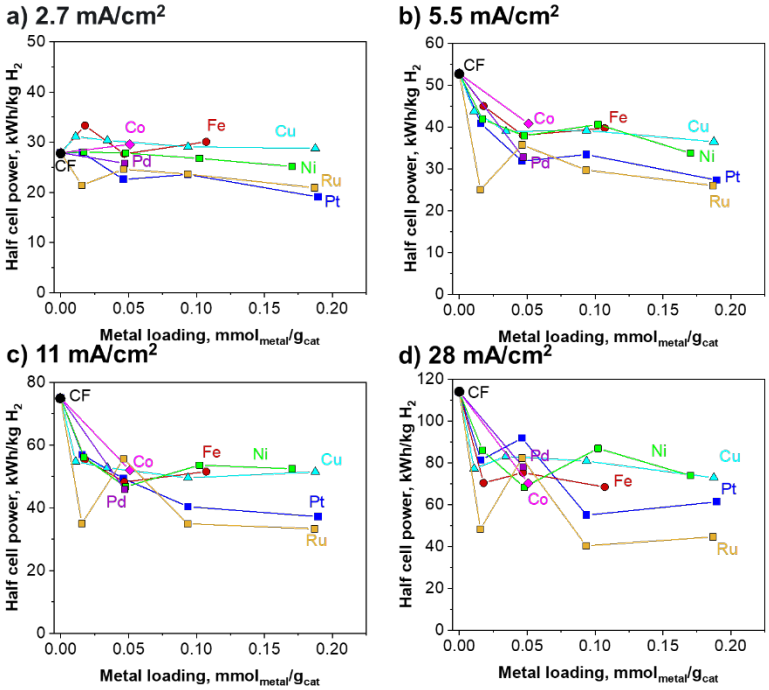

Figure 4.5. Performance for PNNL cathodes for H_2 production using real food waste-derived 5X diluted PHW with 0.1 M NaH_2PO_4/Na_2HPO_4 as a function of current and electrode (cathode) composition. The anode was a PNNL proprietary material. All the cathodes were synthesized with equimolar metal loading, the difference on final metal weight loading content was caused by the changes in molecular weight. The results were obtained in single-pass configuration using flow rates of 4-10 scm^3/min.

4.5.TEC cathode performance using different metals

We have explored the electrochemical performance of different BGM- and PGM-based electrodes at different current densities (2.7 to 28 mA/cm^2). We focused on changing the metal loading (from 0.01 to 0.20 mmol $_{metal}/g_{cat}$) to lower the power required to generate H_2 in a real food waste-derived PHW sample, but 5X diluted and buffered with 0.10 M NaH_2PO_4/Na_2HPO_4. As shown in **Figure 4.5**, the electrodes containing BGM (Ni, Cu, and Co) performed similarly to those with PGM (Pt, Ru, and Pd) but the PGMs provided a bigger decrease in half-cell power for H_2 generation for all the electrochemical conditions tested. Overall, increasing the molar loading decreases the half-cell power but not proportionally, suggesting that there is structure sensitivity (i.e., metal particle size) effects. That is, the morphology of the metal nanoparticles changes with loadings, which in turn changes the intrinsic specific rate.

4.6.TEC performance under different HTL-derived PHW

We have continued exploring the electrochemical performance of the baseline TEC system using different PHW to understand the effect of compositions on the performance. As shown in **Figures 4.6 to 4.8**, the PHW composition or organic and inorganic species can change by up to an order of magnitude. While the COD, TC, TN, and NH_3 are directly converted during the electrochemical reaction, the ions, and cations (**Figures 4.7 and 4.8** respectively) indirectly affect the electrochemical performance as well as the conductivity and pH. We expect that ions and cations are also responsible for the anode deactivation. Hence, we evaluated the effect of ions and cations on the electrochemical all the samples by diluting all the samples, so the concentration of COD was similar across the different feedstocks.

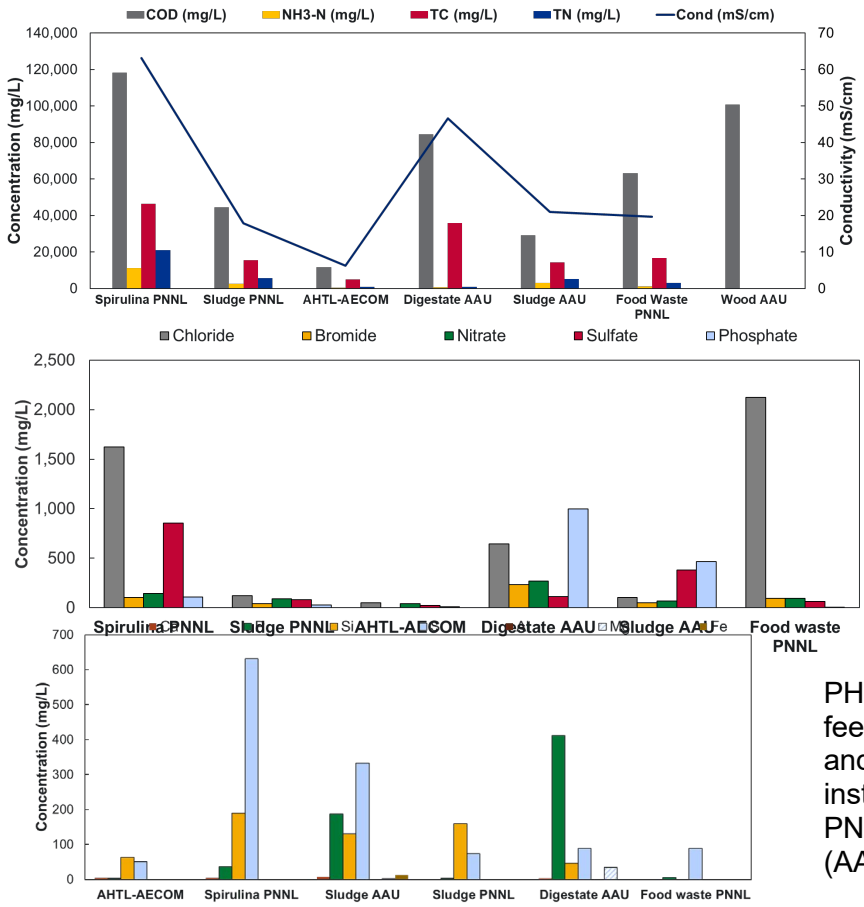

Figure 4.6. Composition of different PHW obtained from different feedstocks (e.g., algae, food waste, sludge, and wood) and different institutions such as AECOM, PNNL, and Aalborg University (AAU).

Figure 7. Comparison of anion concentration in PHW obtained from different feedstocks (e.g., algae, sludge, and wood) and different institutions such as AECOM, PNNL, and Aalborg University (AAU).

Figure 8. Comparison of anion concentration in PHW obtained from different feedstocks (e.g., algae, sludge, and wood) and different institutions such as AECOM, PNNL, and Aalborg University (AAU).

We first evaluated the effect of electrochemical performance of anodes (for COD removal) and cathodes (for H_2 production) as a function of PHW. **Figure 4.9** summarizes the performance the cathode than the anode when using the different PHW compared against that of a clean buffer solution without organics. The half-cell potentials between -1.0 and -1.3 V vs. Ag/AgCl, the performance of the PHW was similar to that of the blank (AlkPBS) performance except for Sludge PNNL sample, which showed 2X higher current density. At potentials more negative than -1.3 V vs Ag/AgCl, other PWH demonstrate higher performance than the blank.

However, the anode had 2X lower activity with all the PHW compared to the blank (Alk PBS), which is consistent with our previous work showing that the oxidation of

organics is a slower kinetic step (i.e., produces a lower current) than the water electrolysis. However, at anode potentials higher than 2 V vs Ag/AgCl, the difference in anode activity obtained with PHW and blank start to decrease.

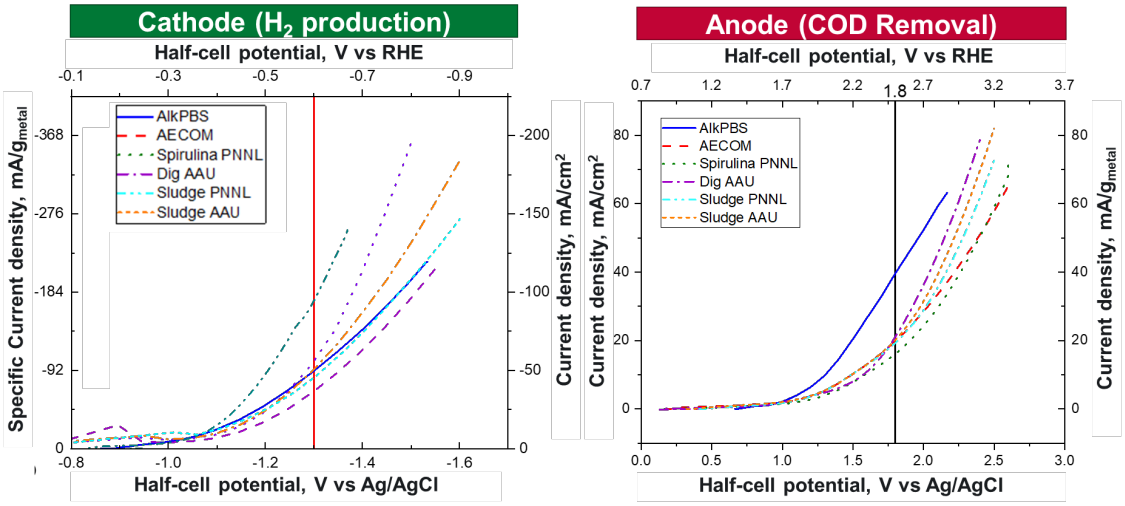

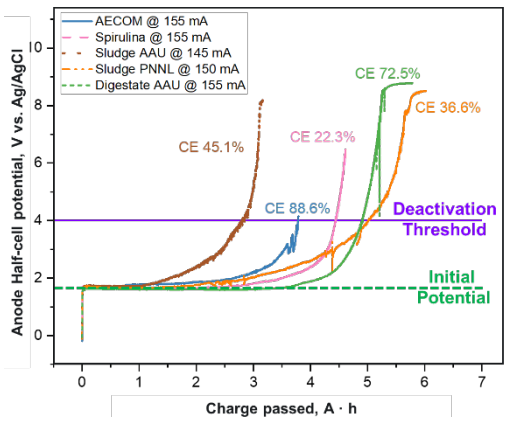

Figure 9. Performance for PNNL' proprietary TEC electrodes in batch cell as a function of half-cell potentials for different compositions of PHW. All the PHW were diluted to have a constants COD level of ≈ 12,000 ppm and contain an equimolar concentration of buffer to keep pH constant during the experiment.

Figure 10. Performance for anode in continuous-flow cell operating at initial constant half-cell potential of 1.8 V vs Ag/AgCl using different PHW with constant COD levels of ≈ 12,000 ppm and 0.1 M of buffer. CE represents current efficiency towards COD removal instead of water electrolysis.

4.7.TEC performance in continuous-flow cell using different PHW

We evaluated the performance of the TEC anode and cathodes in continuous-flow cell to determine the long-term stability, and energy cost of the for the simultaneous COD removal and H_2 production from different PHW. As shown in **Figure 10**, the stability experiment with the different PHW started at the same potential (1.8 V vs Ag/AgCl); however, the charged passed before the electrode deactivated (i.e., the potential increases to generate a constant current) changed by nearly a 4X. Additionally, the current efficiency (CE) for COD removal over water splitting also changed with the PHW composition. Hence, these results suggest that even when having constant COD concentration, the PHW composition will the electrode stability.

Table 1 summarized the performance of the TEC with the different PHW and reveals that the power required to remove COD changed by 4X (from 88.6 to 22.3 kWh/kg COD), while The H_2 production rates were only affected by 20% (from 108 to 88.5 kWh/kg H_2). Again, these results suggest that the anode is the most affected by the PHW composition while the cathode performance is not. Additionally, while the same anode was replaced after each experiment, the same cathode was used for all the experiments and no signs of deactivation was observed.

Even though the COD removal and H_2 production are two parallel reactions, the power consumption calculations assume the whole power of the electrolyzer to better compare against the state-of-the-art technologies (i.e., anaerobic digestion for COD removal and water electrolysis for H_2 production). However, we would like to highlight that the same power performed both reaction; hence, if the users pay the 22.3 kWh//kg COD, the produced H_2 has no electrical cost. Likewise, if the user pays for 88.5 kWh/kg H_2, the COD removal has no electrical power cost.

Table 1. Summary of performance of the TEC flow system using different PHW.

PWH	Charge To Failure, C	COD Removal, kWh/kg COD	CE for COD Removal, %	H_2 Production, kWh/kg H_2	Faradaic Efficiency (FE) for H_2 production, %	kg H_2 Prod./ kg COD Rem.
AECOM	13,950	16.6	88.6	94.9	100	0.175
Spirulina	12,834	60.8	22.3	96.1	100	0.633
Sludge AAU	11,484	43.2	45.1	99.8	100	0.433
Sludge PNNL	21,600	60.8	36.6	108	89.5	0.563
Digestate AAU	20,646	37.1	72.5	86.8	100	0.427
Wood AAU	23,310	63.7	21.1	88.5	92.7	0.720

4.8.TEC long term stability performance

We evaluated the long-term stability of the TEC system under different electrochemical reactions conditions. As shown in **Figure 4.11**, the Full-cell power (including both anode and cathode) and the stability of the TEC system depended on the current density. At low current densities, the TEC operate for over 600 h without apparent deactivation and had the lowest power requirements, 68.4 kWh/kg H_2. However, the system showed deactivations within 40 h when operating at 17 mA/cm^2 at had the highest

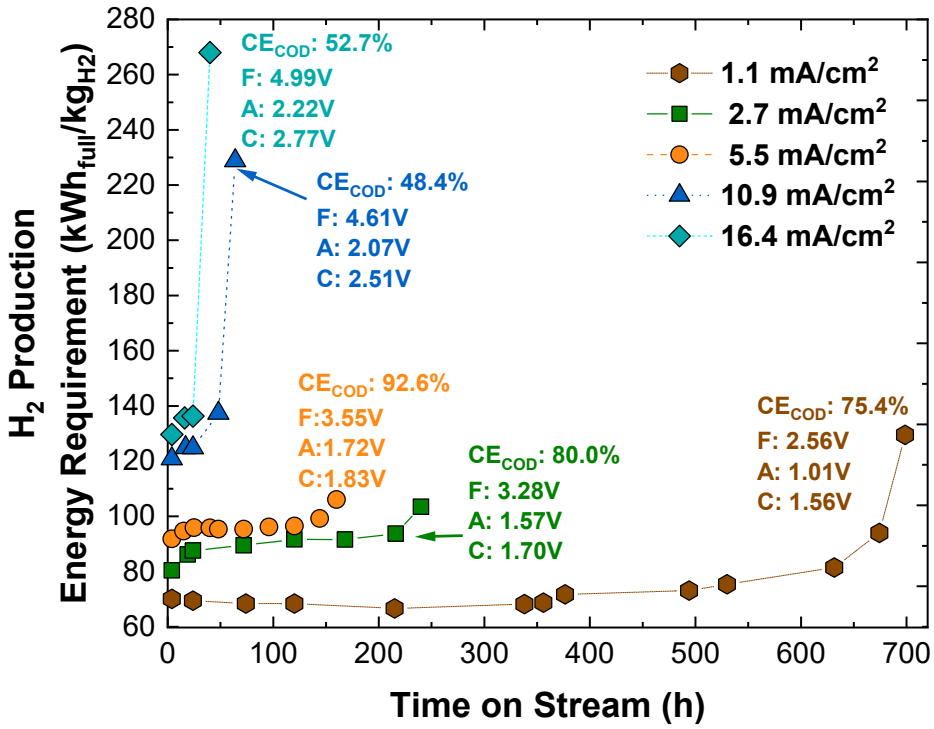

Figure 11. Performance for PNNL' TEC when operating at different current densities using real food waste-derived 5X diluted PHW with 0.1 M NaH_2PO_4/Na_2HPO_4. The anode and cathode are PNNL proprietary material. The results were obtained in continuous-flow electrolysis cell operating in full recycle and using flow rates of 4-10 scm^3/min. F represents full cell potential, A represents anode half-cell potential vs RHE, and C represents cathode half-cell potential vs RHE. CE_{COD} represents the current efficiency for COD removal.

power requirements, 136 kWh/kg H_2. The Milestone of 100 h stable performance was achieved at current densities of 1.1, 2.7, and 5.5 mA/cm^2. Analysis of the electrodes showed that the reason for the deactivation was anode degradation. After replacing the anode, the cell and cathode performed equally suggesting that both the membrane and cathode did not degrade.

Task 5: Pilot MEC development and Integration with HTL for Testing and Analysis (Lead; Princeton Ren Group)

5.1. MEC scale-up configuration

To scale up the MEC, we first conducted a comprehensive literature review on existing scale-up efforts. We compared the major scale-up configurations and systematically evaluated their performance from both technical and economic perspectives. We characterized how system scale-up impacts the key performance metrics such as volumetric current density and H_2 production rate. Drawing from this experience, we designed modular pilot cells to integrate onsite with pilot HTL system. Long-term single pilot reactor operation revealed that fixed anode potential enabled rapid startup, and low catholyte pH and high salinity were effective in suppression of cathodic methanogenesis and acetogenesis – resulting in high current density of 16.6 A/m^2 and 9.3 A/m^2 when feeding synthetic wastewater and PHW respectively. Additionally, the anode biofilm exhibited spatial variations in response to local environmental conditions. Onsite parallel or serial operations of multiple pilot MECs showed good performance using actual PHW with a record-high H_2 production rate of 0.5 $L/L_R/day^{-1}$ for MEC over 300 liters scale, and the optimal chemical oxygen demand (COD)-to-H_2 yield reached 0.127 kg-H_2 per kg-COD, supporting a self-sufficient, closed-loop upgrade to jet fuel.

Many groups have reported their pilot MEC configurations, but they can be divided into two major categories: reactor-based or electrode-based modularization (**Fig. 5.1**)[13]. The concept of reactor modularization was realized by hydraulically connecting several reactor units in series or in parallel to achieve a higher overall volume. When connected in series, the hydraulic retention time was maximized, which could lead to better organic removal, but the treatment capacity was limited. When connected in parallel, treatment capacity and overall H_2 production could be increased, but the wastewater treatment efficiency may be limited. Therefore, there is no single optimal configuration, and the selection of configurations should depend on the priority of the design and operation. We compared the major scale-up configurations and systematically evaluated their performance from both technical and economic perspectives. We characterized how system scale-up impacts the key performance metrics such as volumetric current density and H_2 production rate, and we proposed methods to evaluate and optimize system design and fabrication.

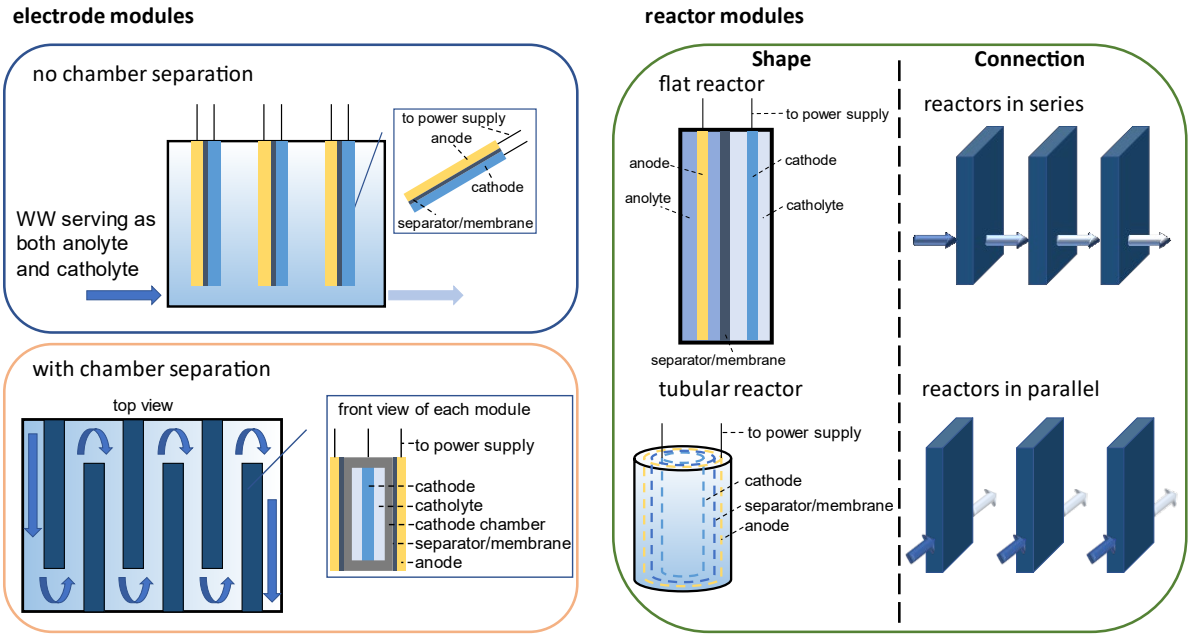

Figure 5.1. Different modularization methods used in pilot MECs. WW = wastewater.

5.2. In-Lab Pilot MEC construction and operation

Build on the successful lab research on validating the feasibility of MEC PHW treatment, deciphered the degradation mechanisms, and analyzed the MEC scaleup state-of-the-art, we designed our pilot reactors at 80 liter scale each and operated the MECs in the lab to identify keys and challenges, and to verify the long-term stability. In total, four reactor modules were manufactured, one for in-lab long-term operation (R-single), and three for onsite operation (R1-R3). Each reactor module (110 cm×13 cm×60 cm) came in rectangular shape with reactor frames manufactured from acrylic. Each module was divided into three chambers with two anode chambers (100 cm×4 cm×50 cm each) on the side and one cathode chamber (100 cm×3 cm×50 cm) in the middle. Two back plates

(each 1 cm wide) enclosed the chambers by sandwiching the two anode chamber frames and one cathode chamber frame in between. Nineteen carbon brush anodes (60 cm long with 10 cm bare end and a carbon brush diameter of 4 cm) were evenly inserted into each anode chamber and were connected by wire connector blocks (Jandeccn) through 14-gauge wires. Before insertion, the carbon anode brushes were heat-treated at 450 ℃ for 30 min. Stainless steel wire cloth (316 SS, 60×60 mesh size, 0.009" opening size, McMaster-Carr) were used as cathode. The wire cloth was cut into 78 cm×26 cm size (2,000 cm^2 cross section area) and fixed with titanium wire (0.031" Diameter, 1/4 lb. Coil, McMaster-Carr) for connection with potentiostat and power supply. The anode chamber and cathode chamber were separated by cation exchange membrane (CXM-200, Membrane International Inc.) Two different types of PHW were produced and tested in the study, one from grocery food waste collected from a local grocery store in Champaign, IL (PHW-GFW) and one from salad dressing waste collected from local food processing plant (PHW-SDW). The PHW characterization is summarized in **Table 5.1**.

Table 5.1. PHW characterization of the two PHW feedstocks used in this study

Parameters	Unit	PHW-GFW	PHW-SDW
COD	mg L^{-1}	110,880±1,018	41,200±1300
Total Nitrogen	mg L^{-1}	8,490±1,367	469±19
NO_3-N	mg L^{-1}	87.6±6.2	350±12
NH_3-N	mg L^{-1}	2,760±102	26±3
ORG-N	mg L^{-1}	5,642±1,258	93±4
Glycerol	mg L^{-1}	8,492±101	2,058±30
Acetate	mg L^{-1}	3,938±98	1,269±57
Ethanol	mg L^{-1}	7,139±187	20±1
pH		5.1±0.1	3.7±0.1
Conductivity	mS cm^{-1}	33.1±0.2	16.3±0.1

The R-single reactor demonstrated strong performance under varying operational conditions, achieving a maximum current density of 16.6 A/m² with synthetic wastewater and 9.3 A/m² with PHW-GFW (**Fig. 5.2**). While slightly lower than the 20 A/m² observed in prior lab studies with PHW, these values exceed those of most lab-scale microbial electrolysis cells (MECs), which typically achieve <10 A/m². These results are notable given the reactor's use of a low-cost stainless-steel cathode, which performed comparably or better than expensive catalysts. High current density was attributed to the anolyte's conductivity, a known positive correlate, despite challenges with PHW-GFW due to its complex substrate composition, including glycerol and nitrogen-containing heterocyclic compounds.

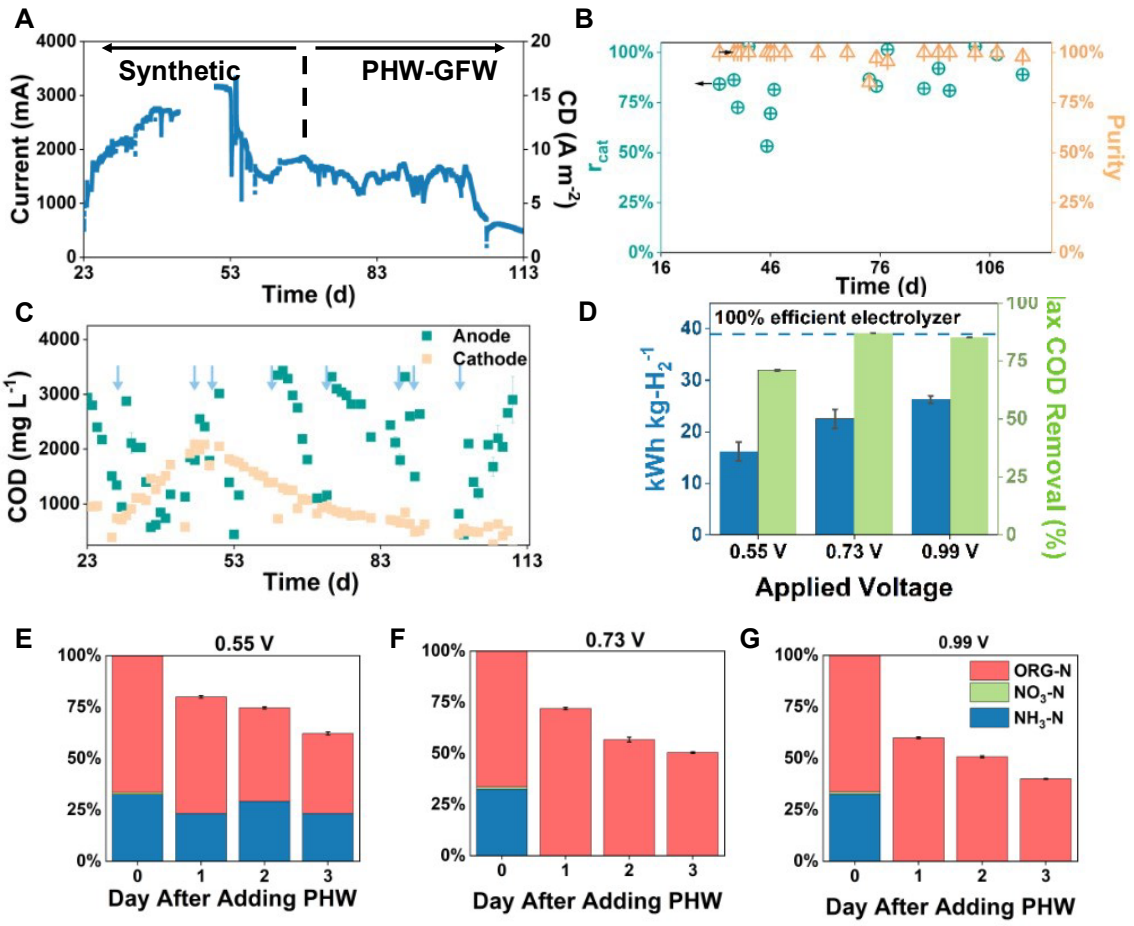

Fig. 5.2. Long-term in-lab operation of R-single. (A) Current density profile. The data file between Day 43 - 51 was lost due to a computer power issue. The power cutoff did not affect the power supply, therefore the reactor was operated as usual. CD: current density; (B) r_{cat} and purity of H_2 in the cathodic gas; (C) The anode and cathode COD profile, the blue arrow indicates the dosing of fresh substrate; (D)The energy consumption for H_2 production and the maximum COD removal under different voltages. The blue dashed line represents the minimum energy consumption of water electrolysis. The degradation profile of nitrogen species under an applied voltage of (E) 0.55 V, (F) 0.73 V and (G) 0.99 V. The y-axis is normalized to the initial nitrogen concentration.

COD removal efficiency was consistently high. Synthetic wastewater achieved >60% COD removal within a week, with peak kinetics reaching 85% within three days (days 50–53). For PHW-GFW, despite slower kinetics, the reactor achieved >70% COD removal at 0.55 V and >85% at higher voltages (0.73–0.99 V). Notably, applied voltage was measured directly to account for ohmic losses, significant in larger-scale systems.
The reactor achieved low energy consumption, a critical advantage of MECs over abiotic electrolysis for H_2 production. At 0.99 V, energy consumption was 26 kWh/kg-H_2, roughly half that of state-of-the-art water electrolyzers (~50 kWh/kg-H_2). At 0.55 V, energy consumption further dropped to 16 kWh/kg-H_2. This efficiency underscores the potential for reduced costs, as electricity dominates electrolysis expenses.

Nitrogen removal efficiency was voltage-dependent, with nearly complete NH_3-N removal at 0.73–0.99 V, while organic nitrogen (ORG-N) removal remained low (24–40%). The Maillard reaction compounds in PHW limited ORG-N degradation, necessitating a downstream polishing step to meet discharge standards. The findings highlight the reactor's effectiveness and scalability potential, with ongoing challenges in ORG-N treatment requiring additional innovations.

5.3. Onsite Integration of HTL and MEC

The pilot MECs were integrated with an onsite HTL reactor under temperature-controlled conditions to maintain microbial activity. Due to the winter weather, the MEC reactors were housed in a tent with temperature control to maintain microbial activities (**Fig. 5.3**). To reduce pipeline blockage and membrane fouling, the raw PHW was pretreated with bag filter to remove the oil chunks prior to pumping into the MEC modules. In onsite-integration, two operational modes were tested after successful start-up: in-series and in-parallel (**Fig. 5.3**)[14]. The operational modes refer to the anodic loop, as the cathodic loop was always run in parallel with 100% recirculation. The overall HRT in both operational modes were controlled at 72 hr to provide a fair comparison under the same treatment capacity. In other words, the flow rate for each module under in-series mode was three times as fast as in in-parallel mode.

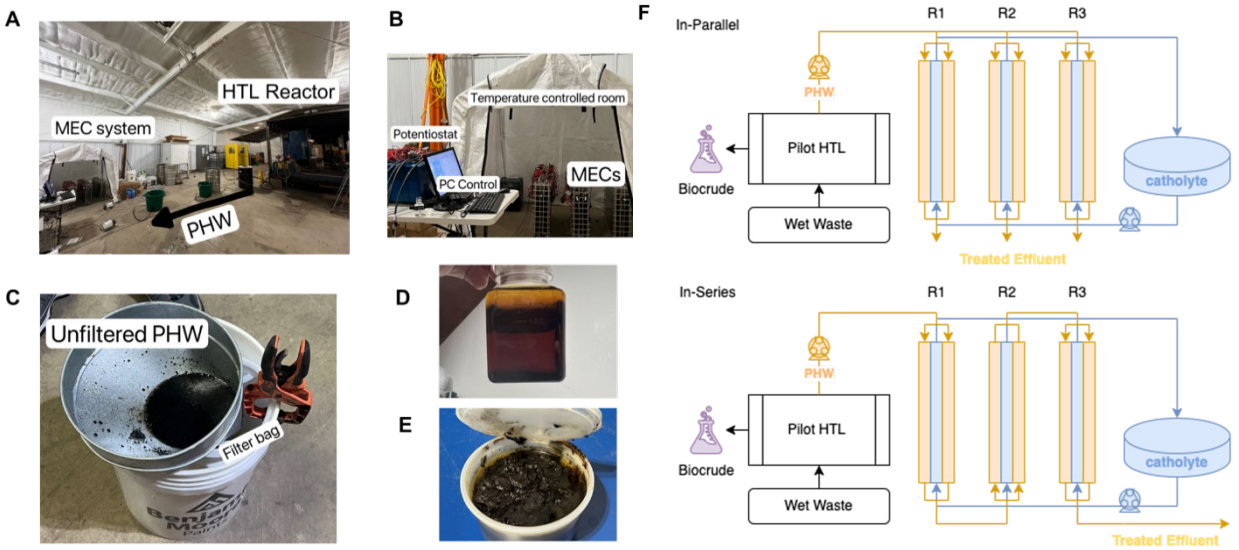

Fig. 5.3. Onsite operation conditions and test modes. (A) Picture showing the inside of the building which houses the pilot HTL and MEC systems; (B) Picture of the MEC system; (C) Picture showing the pretreatment process to remove the suspended solids; (D) Filtered PHW; (E) Oil chunks from the filter bag; (F) Two operational modes explored in onsite integration.

During synthetic wastewater acclimation, the reactors reached current densities >1 A/m² within three days, facilitated by optimal conditions (30°C, preacclimated inoculum, and anode potential of -0.35 V vs Ag/AgCl). Switching to PHW-SDW diluted to 5,000 mg/L COD, the reactors demonstrated reliable performance (**Fig. 5.4**). In-parallel operation

achieved a maximum current density of 8.7 A/m². In-series operation showed tiered current density, with R1 reaching 12.5 A/m². COD removal during in-series mode was higher (up to 86.4%) than in-parallel mode (maximum 66.3 ± 10.6%), attributed to better mass transfer and extended retention time.

Hydrogen (H_2) production rates followed current density trends, with r_cat consistently >90%. Using synthetic wastewater, the maximum H_2 production rate was 1.1 L/Lcat/day, which increased to 1.8 L/Lcat/day for R1 during in-series operation with PHW-SDW. This performance represents the highest H_2 production rate reported for pilot MECs >10 L, with normalized production reaching 0.5 L/LR/day. Achieving these results required maintaining cathodic pH at 4, which reduced energy requirements by 0.18 V but introduced operational costs.

A critical objective was evaluating whether MEC-produced H_2 could meet the demand for biocrude upgrading in a closed-loop system. For a yield of 0.098–0.109 kg-H_2/kg-COD (threshold for closed-loop upgrading), the average yield during in-series operation was 0.058 kg-H_2/kg-COD, falling short due to variations in Coulombic efficiency (CE). However, in-parallel operation exceeded the threshold, achieving a yield of 0.127 kg-H_2/kg-COD, surpassing the theoretical maximum (0.125 kg-H_2/kg-COD) due to measurement margins of error. The high yield in-parallel mode was achieved without compromising r_{cat}, indicating effective COD degradation by electroactive microbes.

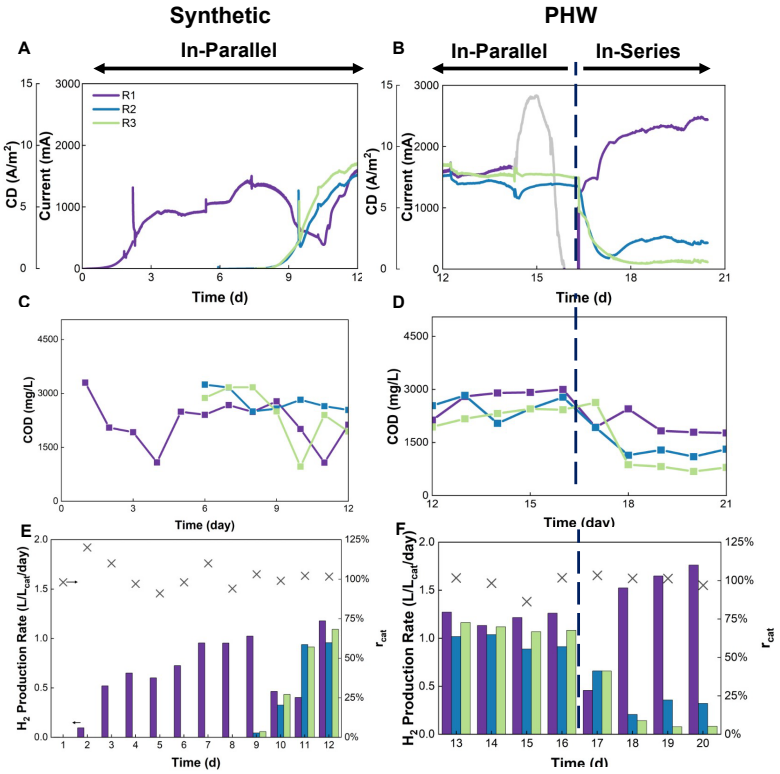

Fig. 5.4. Onsite integration results. Current profile during operation on (A) synthetic wastewater and (B) PHW in both operation modes. The greyed-out data in panel B indicate invalid data from resistor failure on R1; COD profile during operation on (C) synthetic wastewater and (D) PHW in both operation modes. COD samples were taken from effluent of each module; H_2 production and r_{cat} during operation on (E) synthetic wastewater and (F) PHW in both operation modes. Note that R2 and R3 were started one week after R1.

In summary, we successfully carried out lab-scale and pilot scale MEC operation for PHW treatment and valorization and successfully met all the proposed milestones. We achieved 1.62 L/L/day H_2

production rate, operated a pilot MEC in lab for 3 months, and operated onsite pilot totaling > 700 L of conditioned PHW treated. Both the lab-scale and pilot-scale achieved record-high H_2 production rate for MEC reactors running on PHW at the corresponding size range. MEC were tested on a range of different PHW coming from different substrates, and all exhibited satisfactory performance. We also established the first anode metabolic network for MEC treatment of PHW.

Task 6. TEA Analysis (Lead: Lesley Snowden-Swan, Shuyun Li, PNNL)

6.1: TEA analysis

To explore the performance of conversing food waste to fuel via an integrated T-MEC with HTL process, techno-economic analysis (TEA) was conducted estimate carbon yield, energy requirements, jet fuel production, and capital and operation costs. Also, a sensitivity analysis was performed to identify key cost drivers and possible areas of optimization towards achieving 1) 50% improvement in carbon efficiency and 2) 25% reduction of disposal.

We started to develop rigorous process model in Aspen Plus 10® by leveraging our in-house large-scale sludge HTL models and the available PNNL's continuous food waste HTL run data. The food waste sample was collected from local dining facilities at Joint Base Lewis-McChord (JBLM), WA with the 25.7% solid content (including 4.3% ash). **Table 6.1** summarized the data of the food waste and the derived biocrude and hydrotreated oil.

Table 6.1. The experimental data summary of food waste, biocrude and hydrotreated oil

	Food Waste	Biocrude	Hydrotreated Oil
Carb/Fat/Protein/FAME	54.1/21.0/21.7/16.8		
Yield, wt%	-	45.6	84
C	54.1	76.3	85.1
H	8.0	9.7	13.5
O	36.0	10.3	0.2
N	3.5	3.5	1.1
S	0.2	0.3	0.0

Identifying chemicals in the derived biocrude and aqueous phase is very critical to the model accuracy and TEA results. Thus, we examined over 500 identified chemicals in biocrude via GCMS and compiled them into several groups such as hydrocarbon, N-, S-, O-containing organics, amide, and acid. Then select the high-content chemicals for each group as the model chemicals implemented in our process model. Note that GCMS can only identify about 67%C, 80% H, 74% O and 15% N in the biocrude and the unknown heavy compounds are represented by two heavy molecules in the model, which as $C_{19}H_{16}N_4$ and $C_{24}H_{30}O_4$. **Table *6.2*** shows the selected high-content model chemicals and its normalized percentage by weight in biocrude.

Table 6.2. The experimental data summary of food waste, biocrude and hydrotreated oil

Type	Chemical Name	Formula	wt%
S-organic:		C5H9NS	
CxHy:	Toluene	C6H6	0.27%

	Ethylbenzene	C8H10	0.14%
	Heneicosane	C21H44	0.34%
N-organic:	1H-Pyrrole, 3-ethyl-2,4,5-trimethyl-	C9H15N	1.17%
	Indolizine	C8H7N	0.21%
	Pyridine, 2-methyl-	C6H7N	0.09%
	Pyrazine, methyl-	C5H6N2	0.30%
	Benzonitrile, 2,4,6-trimethyl-	C10H11N	0.23%
O-organic:	Phenol	C6H6O	0.57%
	Cyclopentanone	C5H8O	0.23%
Amide:	Hexadecanamide	C16H33NO	4.75%
	9-Octadecenamide, (Z)-	C18H35NO	4.57%
	Pyrrolidine, 1-(1-oxo-9-octadecenyl)-, (Z)-	C23H43NO	0.98%
Acid:	n-Hexadecanoic acid	C16H32O2	25.24%
	Octadecanoic acid	C18H32O2	60.91%

Similarly, the model chemicals in aqueous phase are identified and corrected in the Aspen model with the help of GCMS, HPLC, elemental composition as well as the property data such as total carbon, total nitrogen, COD and NH3 content. **Table 6.3** list the comparison between the modeled results and experimental data.

Table 2.3. The modeled results vs. experimental data for the aqueous phase

	Modeled Result	Experimental Data
TOC in total Aq.	2.30%	-
TC in total Aq.	3.03%	2.31%
TOC/TC Ratio	76.0%	-
CO_2	0.91%	-
TC	0.52%	0.51%
NH_3	0.30%	0.14%
COD, mgO/L	65272	68500
Acetic acid	0.707%	0.60%
Butanoic Acid	0.078%	0.05%
1,2-Butanediol	0.022%	0.01%
Ethanol	0.516%	0.49%
Propanoic Acid	0.371%	0.14%
Glycerol	0.847%	0.54%
Ethylene Glycol	0.050%	0.03%
1,3-propanediol	0.998%	0.21%
Produced water	1.20%	-
p-Cresol	0.22%	0.00%

6.2: Carbon Conversion for Benchmark Anaerobic Digestion System. TEA Approach and Economic Assumptions.

A discounted cash flow and internal rate of return (IRR) approach were used to evaluate the minimum fuel selling price (MFSP) in 2020 U.S. dollar basis, which is the cost of production that causes a zero net present value with a fixed IRR. The MFSP was normalized to $/gasoline gallon equivalent (GGE) basis by applying the lower heating value (LHV) of gasoline. The variable cost was calculated from the mass and energy

balance and prices of raw materials and utilities. The process models developed in AspenPlus was used to calculate the mass and energy balance. Capital cost of major equipment was calculated from Aspen Capital Cost Estimator and/or vendor costs whichever was available. Producer price index (PPI) for chemical manufacturing, labor index for chemicals production workers from the U.S. Bureau of Labor Statistics, and the Chemical Engineering Plant Cost Index (CEPCI) from Chemical Engineering were used to escalating the original price quote at different year basis to the 2020 U.S. dollar basis. Tables X.1 and X.2 listed the harmonized economic and pricing assumptions.

Table 6.4. Economic assumptions.

Assumption	Value	Assumption	Value
Pricing basis	2020	Plant life (yr)	30
Project contingency (%)	60	Construction period (yr)	3
Indirect cost factor (% of TIC)	18.5	Maintenance/overhead (% of labor)	90
Working capital (% of FCI)	5	Start-up time (yr)	0.5
Depreciation period (yr)	7	Stream factor (%)	90
Equity financing (%)	40	Internal rate of return (%)	10
Loan rate (%)	8	Income tax rate (%)	21

TIC = total installed cost, FCI = fixed capital investment

Table 6.5. Pricing assumptions (in 2020 U.S. dollar).

Utilities	Price
Natural gas ($/1000scf)	3.80
Electricity (¢/kWh)	6.67
Water makeup ($/metric ton)	0.4
Steam (¢/Mlb)	390
Solid disposal ($/ton)	54.8
Wastewater fee ($/metric ton)	1.0

To make fair comparison between the proposed HTL-MEC system and AD, a thorough literature has been made to collect food waste to biogas process data. **Figure 6.1** show the benchmark AD flowsheet. The available food waste to raw biogas carbon efficiency range in the literature is 29%-57% with the average value of 41%. This is mainly due to the food waste composition discrepancy. So, it would be necessary to use the same food waste as the HTL process, which is Joint Base Lewis-McChord (JBLM) with details above. The theoretical carbon efficiency of JBLM to biogas is 52% using the Buswell equation and JBLM food waste to biogas carbon efficiency is 44% if assume 85% theoretical biomethane yield. The carbon efficiency of JBLM to renewable natural gas for vehicle fuel (RNGV) is 35% with a typical of 80% methane recovery rate in gas cleaning.

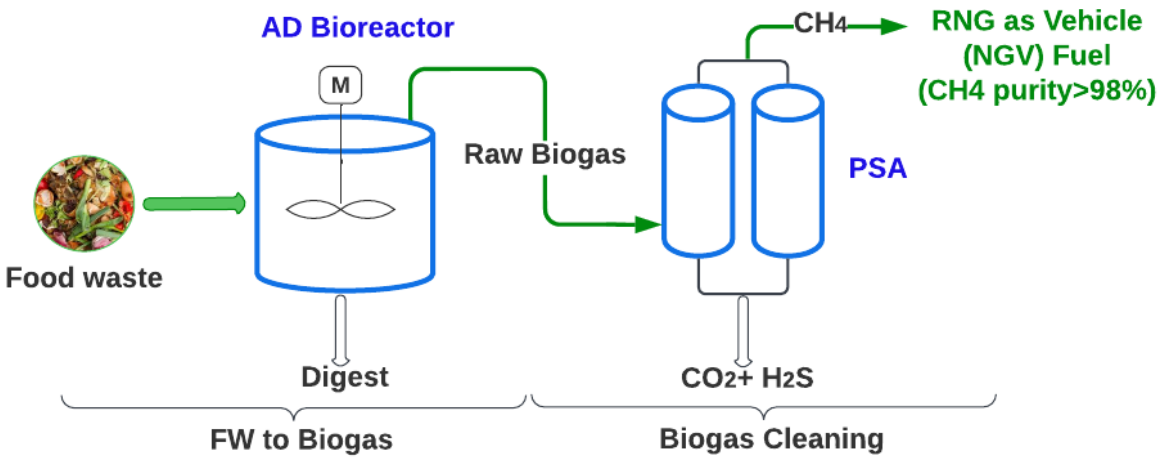

Figure 6.1. Process diagram of benchmark AD system

With the key process assumption and identified chemical models refined in the process model, carbon flow and potential hydrogen consumption was conducted. **Figure 6.1** shows the carbon and nitrogen flow results in the processes. HTL can efficiently convert 60% of the feed carbon to finished oil (SAF, diesel, naphtha) even without any potential carbon contribution from TMEC of aqueous phase. MEC has the potential to efficiently decrease aqueous COD level by converting organics in aqueous to CO_2. For the nitrogen balance, HTL can transfer the majority of N to HTL aqueous (PHW) and biocrude. N in aqueous mainly present in the form of NH_3 and a small fraction in organic N. MEC can convert about 70% N in aqueous to N_2.

Carbon Efficiency Comparison between AD and HTL-MEC

Figure 6.2 summarizes the anaerobic digestion (AD) and hydrothermal liquefaction (HTL) carbon efficiencies based on available literature data and PNNL's bench-scale food waste HTL and biocrude hydrotreating experiments. The dataset includes 12 instances of food waste AD data, primarily sourced from university canteens/cafeterias or local communities. The carbon efficiency of converting food waste to raw biogas ranges from 29% to 57%, with an average of 41%. Similarly, the carbon efficiency for converting food waste to natural gas vehicle (NGV) fuel ranges from 23% to 46%, averaging 33%.

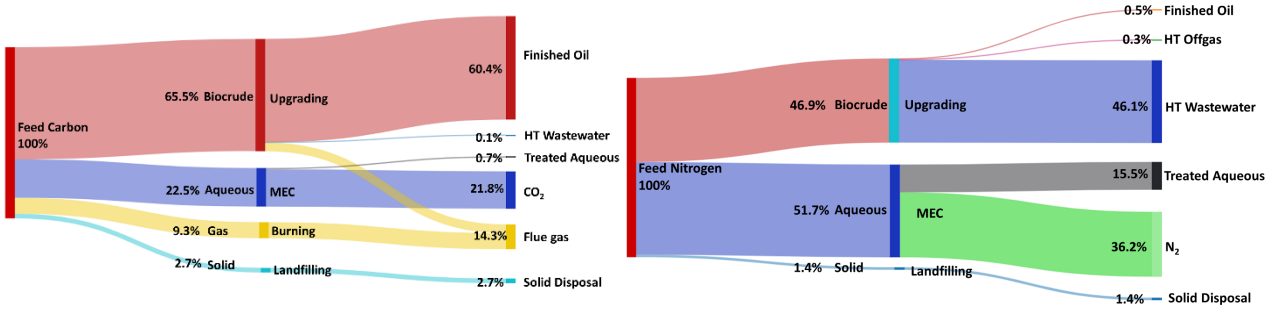

Figure 6.2. Carbon and nitrogen flow distribution over the integrated HTL-MEC process

In comparison, nine datasets of food waste conversion to fuel via HTL-MEC indicate that the carbon efficiency for converting food waste to biocrude ranges from 58% to 74%,

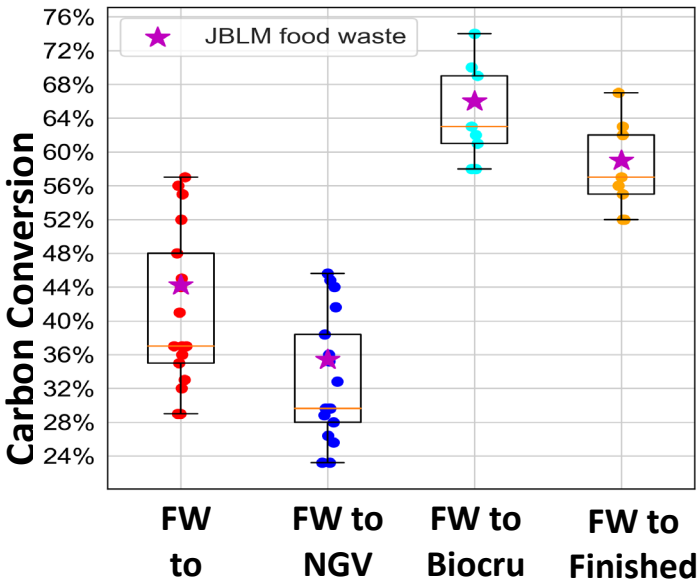

with an average of 65%. The efficiency for converting food waste to finished oil ranges from 52% to 67%, with an average of 58% (**Figure *6.3.***). As shown in **Table 6.5**, whether comparing the same food waste (such as JBLM food waste in this study) or different food wastes from various locations, the HTL-MEC system demonstrates over a 50% improvement in carbon efficiency compared to AD.

Figure 6.3. Carbon efficiency for Integrated HTL vs. Benchmark AD.

Table 6.5. Carbon efficiency summary of Integrated HTL vs. Benchmark AD.

Feedstock	Product	AD	HTL-MEC	Change
different FW (average CCE)	Intermediate (biogas/biocrude)	41%	65%	+58%
	Final fuel (NGV/ liquid fuel)	33%	58%	+76%
JBLM	Intermediate (biogas/biocrude)	44%	66%	+50%
	Final fuel (NGV/ liquid fuel)	35%	59%	+68%

Another key process performance is the hydrogen consumption requirement for the upgrading process. Such shown in **Figure 6.4**, the main hydrogen consumption includes the chemical hydrogen consumption for removing heteroatoms & saturate C-C bonds in the hydrotreater and reducing average molecular weight in the hydrocracker, as well as a small fraction of the purge hydrogen for keeping the high hydrogen concentration. Food waste-derived biocrude tends to be high O, and high N as high contends of acids and amides presents in the raw biocrude, which makes hydrogen consumption tends to be high. Experimental chemical hydrogen consumption for hydrotreating is 0.053 wt/wt wet biocrude while a typical hydrocracking chemical hydrogen consumption is assumed to be 0.0045 wt/wt biocrude. With the assumed above, the total hydrogen consumption is about 15.4 lb/hr for 5 dry ton/day scale. MEC can provide enough hydrogen with 97% COD removal. Additionally, as shown, the recovered waste heat from burning HTL gas & HT off gas can meet the heat duty for preheating feedstock, upgrading process and the residual waste heat is 0.08 MMBtu/hr. (no extra fuel gas for this system).

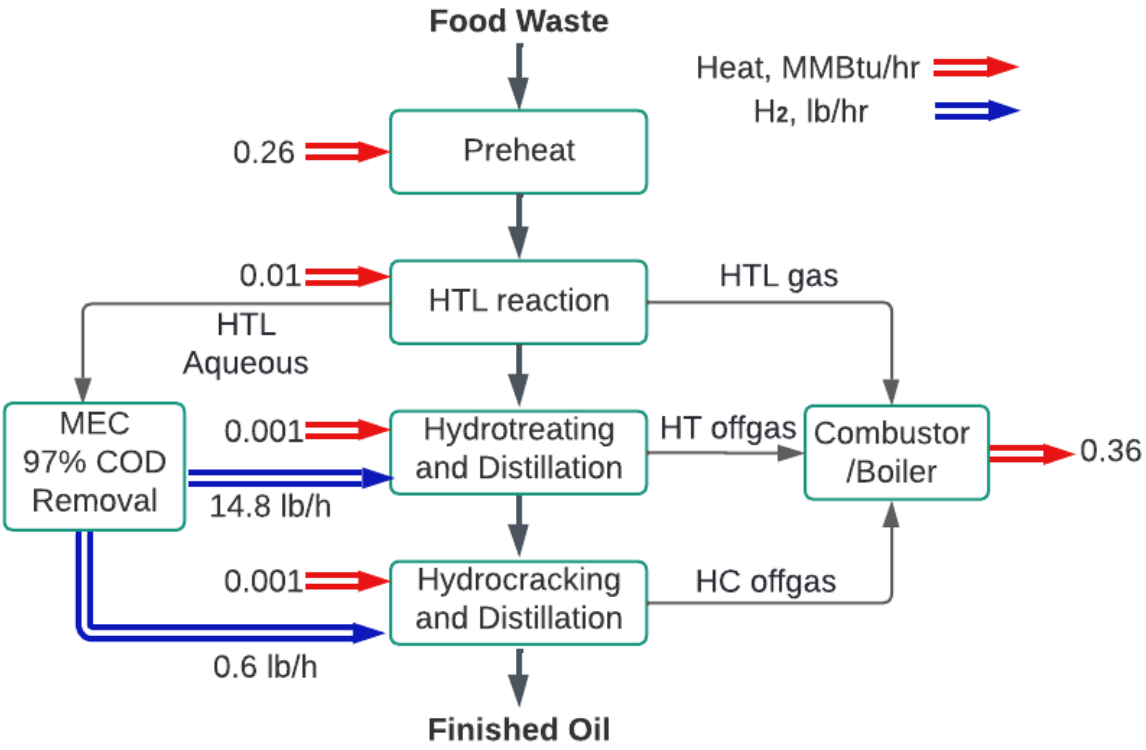

Figure 6.4. Hydrogen and Energy balance for Integrated HTL / MEC-TEC System at 5 Ton/Day.

6.3.TEA of HTL/MEC base case (5 tpd)

The process model and cost sheet for a 5 dry metric ton/day (tpd) integrated HTL with co-located biocrude upgrading plant with TMEC were used as the base case of the TEA study. Based on the current available MEC data, 97% COD removal of HTL aqueous is assumed to meet the required hydrogen consumption. **Table 6.6** shows the current primary MEC parameters for estimating the MEC capital and operating costs. **Table 6.7** shows the economic performance of 5 tpd HTL/MEC integrated system. Note that we assume that the produced hydrogen from MEC is just enough to meet biocrude upgrading requirement and the rest residue COD in the HTL aqueous phase will be discharged to the public wastewater treatment plant with a discharge fee for COD and NH_3. As shown in Table 3.3, it is very challenging to make the small scale HTL/MEC system economically feasible, even for the case only producing hydrotreated oil instead of finished oil (e.g., gasoline, diesel, and jet fuels) to exclude hydrocracking and distillation columns. The hydrotreated oil product could conceivably be sold to a petroleum refinery for co-processing with crude or fractionation into fuels. As shown in Table 3.3, the MFSP for the case of food waste to hydrotreated oil is still in the range of $20/GGE.

Table 6.6. The main parameters for estimating MEC capital and operating costs based on the current lab *scale data*

Parameters	Values	Parameters	Values
Voltage	**1.0 V**	**Current Density**	**1.15 mA/cm^2**
Electricity	**2.83 kWh/kg COD**	**H_2 Production**	**0.098 kg H_2/kg COD**

Diluted COD	2000 mg/L	COD Removal Rate	97%
MEC cost	$225 /m^2	MEC area	16415 m^2

Table 6.7. Plant economics of 5 tpd HTL/MEC integrated system.

	Food waste to finished fuel	Food waste to hydrotreated oil
Installed costs		
Feedstock pretreatment	0.3	0.3
HTL biocrude production	1.8	1.8
HTL Aqueous (PHW) treatment via MEC	3.0	3.0
Hydrotreating	5.2	3.1
hydrocracking	0.7	0
Balance of plant	0.2	0.2
Total installed capital cost	11.2	5.5
Fixed capital investment	21.0	15.6
Total capital investment (TCI)	22.4	16.7
Operating Costs, $/GGE Fuel		
Variable operating cost		
Avoided Feedstock disposal cost	-1.24	-1.24
Chemicals	0.84	0.84
MEC/TEC Maintenance/Replacement	1.18	1.18
Catalyst	0.12	0.12
Waste Disposal	0.13	0.13
Electricity and other utilities	0.69	0.69
Fixed costs	9.08	8.07
Capital depreciation	3.53	2.52
Average income tax	1.04	0.77
Average return on investment	9.65	7.31
MFSP, $/GGE fuel	25.01	20.39
LCOD, $/dry ton waste (with $3.00/GGE fuel)	1,668	1,357
LCOD, $/dry ton waste (with $4.00/GGE fuel)	1,550	1,239

6.3.1.TEA of Benchmark Anaerobic Digestion (AD) System

To improve the comparison between HTL-MEC integrated system with AD system, three different AD scenarios are assumed, as shown in **Figure 6.5**. In particularly, scenario 3 with renewable natural gas (RNG) as vehicle fuel production is very comparable with the liquid fuel from HTL/MEC system. The current available biogas upgrading technologies include water scrubbing, physical adsorption, PSA (pressure swing adsorption), chemical absorption and membrane. In this work, PSA is assumed as the default upgrading process since it can produce high purity methane stream with a simple and compact flowsheet. The produced RNG price is $3.62 MMBTU based on the latest 5 years EIA historic data. The main utility cost is electricity consumption ($10/dry ton waste or $0.0[9]/m3 RNG operating cost is assumed). PSA capital cost with different

plant scale is obtained from open literature, and the regressed relationship between capital cost per capacity and plant scale is shown below:
Capex = 60.826*RNG production rate -0.465
Where the units for capex and RNG production rate are k$/($m^3$/h), and m3/h, respectively.

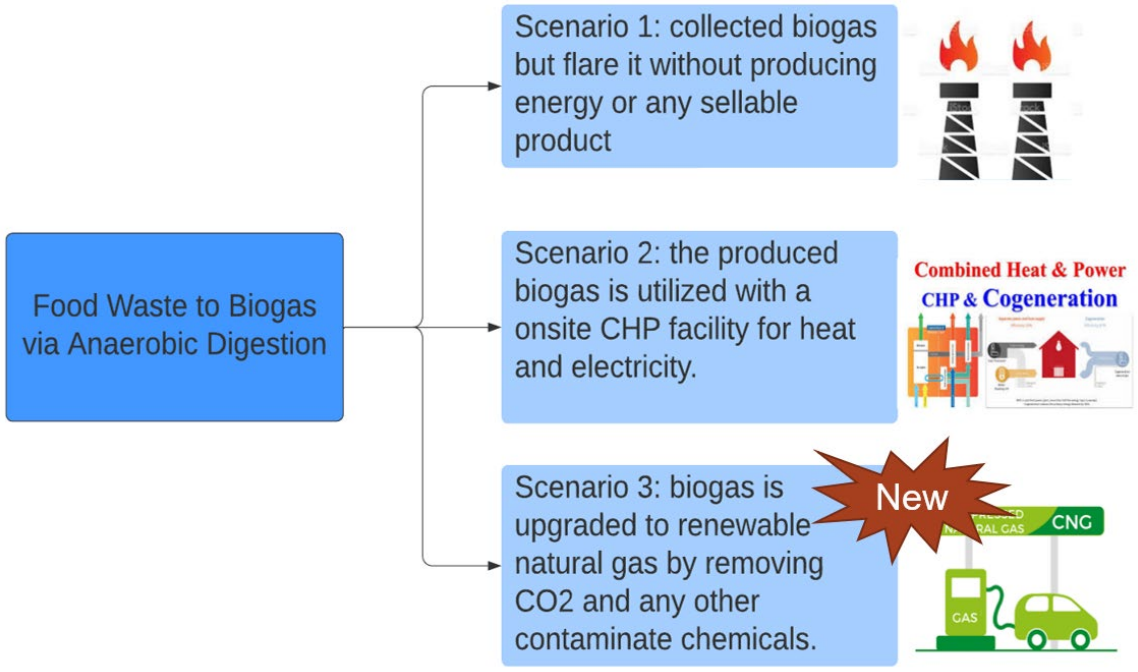

Figure 6.5. Three Benchmark AD: 1) flare biogas without credits; 2) utilize biogas onsite with CHP; 3) upgrade biogas to RNG

With the capital cost and operation cost collected for AD system from open literature, LCOD cost is calculated, shown in **Figure 6.6**. Scenario 1 (flare biogas without credits) has the least capital and operating cost, and it shows cost advantage for the small scale, while Scenario 2 (covert biogas into heat and electricity onsite) LCOD cost is higher than scenario 3 due to relatively low revenue from electricity. Scenario 3 (upgrade biogas to RNG) has the highest capital cost and LCOD steadily reduces with increasing plant scale. For the large scale, scenario 3 has the lowest LCOD cost.

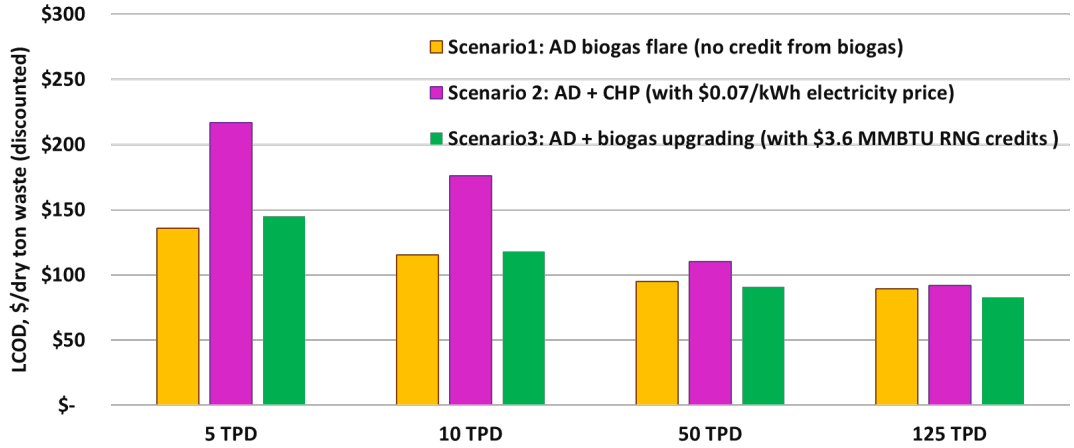

Figure 6.6. LCOD for AD with different biogas utilization scenarios

6.3.2.Sensitivity studies of integrated HTL/MEC plant scale

To illustrate the impact of economies of scale, different scales of integrated HTL/MEC plants are evaluated. **Figure 6.7** show the estimated MFSP and cost allocation by detailed CAPEX and OPEX (**Figure 6.7a**) and by plant area (**Figure 6.7b**), respectively. As shown in **Figure 6.7a**, capital costs and labor contribute nearly 80-90% of the production cost and operating expenses (raw materials, utilities, waste disposal) are only 10-20% of MFSP for the scale bellow 125 tpd. The greater than 125 tpd plant scale, MFSP is close to $ 10/GGE range and the MFSP doesn't decrease much from 125 tpd to 500 tpd. **Figure 6.7b** shows that MEC contributes most for the relatively large scale (> 50 tpd) and MEC CAPEX per capacity is constant regardless of plant scale. Therefore, optimizing MEC system can lead to very competitive MESP, which can be seen from the **Figure 6.8**. Sensitivity of the MFSP of the 500 tpd scale to the variability in process and economic parameters is shown in **Figure 6.8**. As shown, the most significant driver is MEC current density, capital cost, followed by MEC lifetime, feedstock price, MEC buffer consumption, and electricity price. Also, it is noted that MEC method for treating HTL aqueous can be economically competitive with direct discharging HTL aqueous to sewer with tiered fee for the COD and NH_3 level.

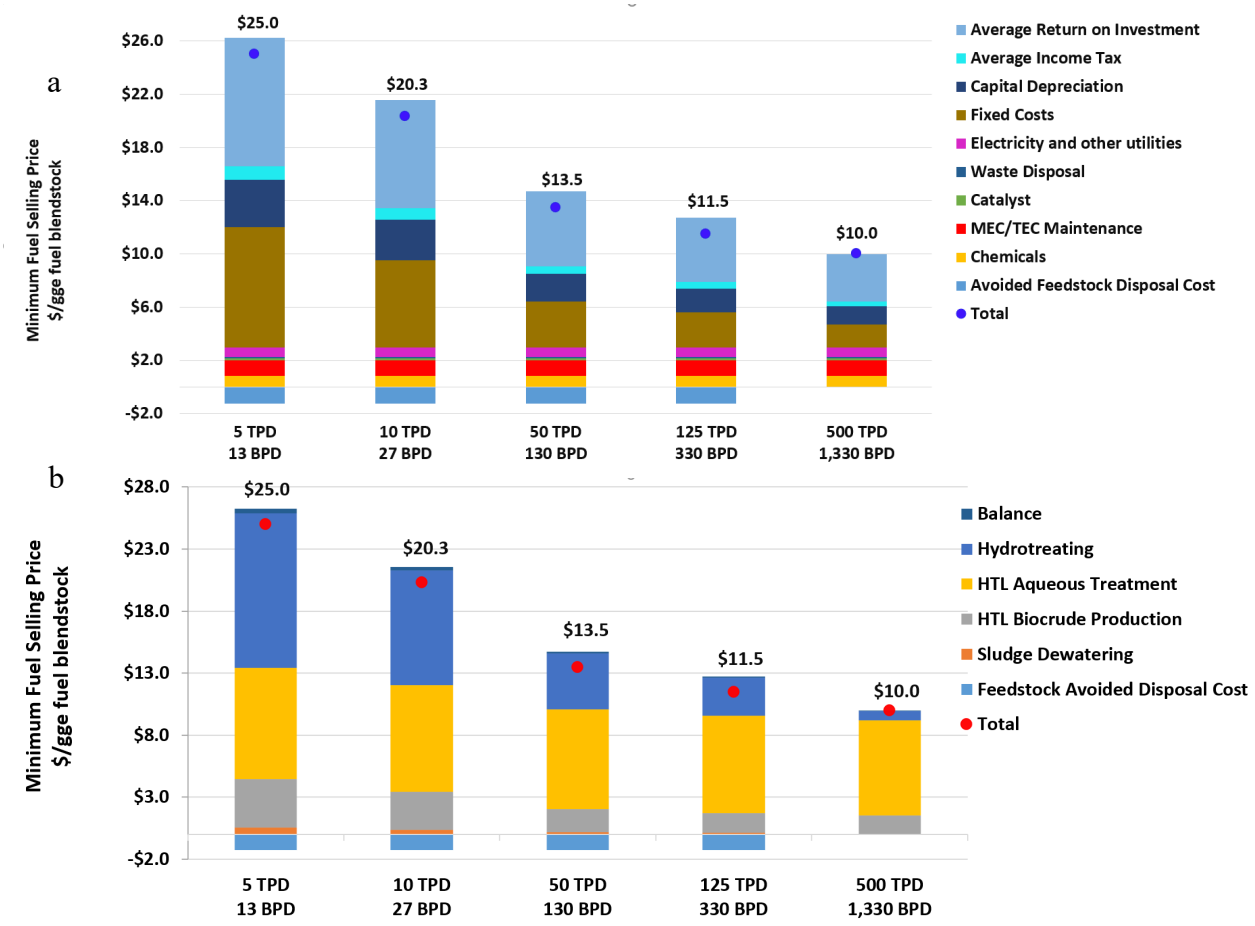

Figure 12. MFSP and cost allocation of different scale of integrated HTL/MEC plant by CAPEX and OPEX (a) and by plant area (b).

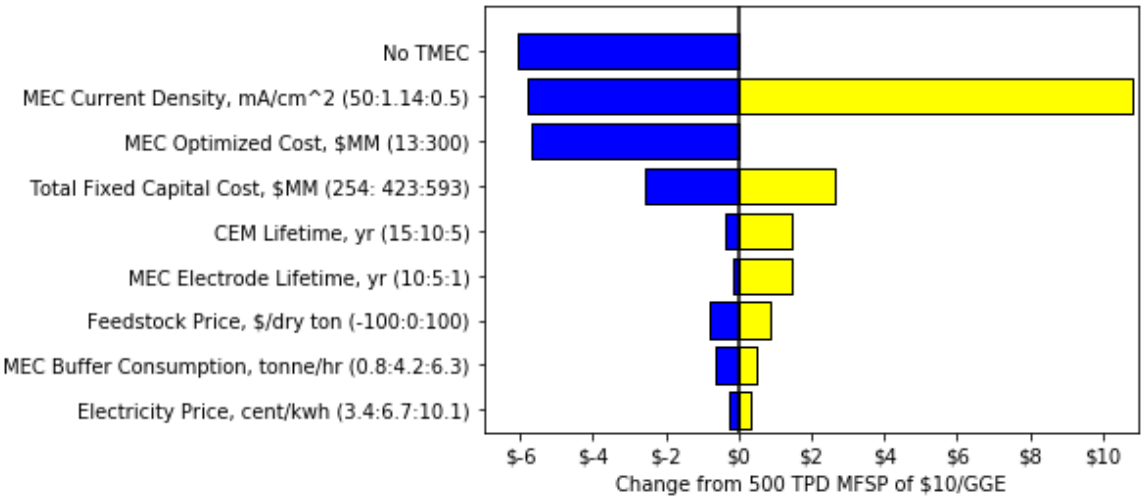

Figure 6.8. Sensitivity of 500 tpd plant's MFSP to various process parameters and economic assumptions.

6.4.TEA of HTL/MEC system with the optimized MEC cost

As mentioned before, the TEA results show that MFSP for community-scale (5 tpd) size plant is $25/GGE and MFSP only dropped to $10/GGE for 100 times community-scale plant (500 tpd) due to MEC capital cost scaling exponent is around 1.0 (MEC capital cost per capacity is constant regardless of scale). Therefore, optimizing MEC capital cost is necessary to lower MFSP. Table 3.4 shows the potential MEC material and cost for the optimized cost based on the vendor's quote on the bulk orders.

Figures 6.9 and **6.10** show the MFSP breakdown for different scales HTL/MEC integrated system. As shown in **Figure 6.9**, optimized MEC with lower capital cost can decrease the MFSP about $5.8/GGE regardless of the plant scale due to MEC scale factor around 1 mentioned above. Specifically, the MFSP decreases from MEC optimization including CAPEX, and MEC maintenance cost, as shown in Figure Y. Note that MEC capital cost and electricity consumption can be further optimized by increasing the current density. The TMEC experimental team targets 5 mA/cm^2 from the current state of 1.15 mA/cm^2.

Table 6.8. The optimized MEC material and capital cost data

	Material	Cost, $/m2
Anode	**Carbon Fiber Brush**	**20/5***
Cathode	**Stainless Steel**	**5/1.25***
IEM/separator	**CEM / Cloth Separator ***	**200/1.25***

* potential material & cost for the optimized case

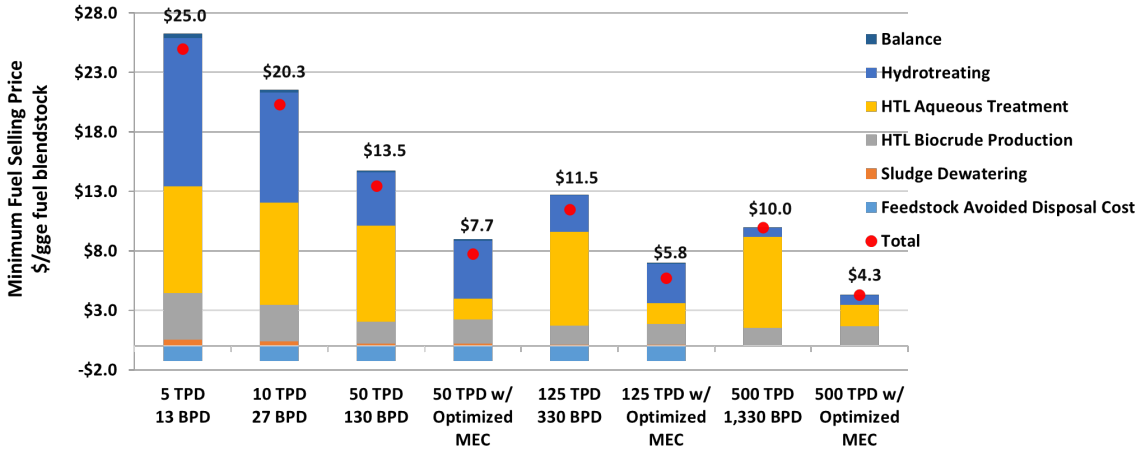

Figure 6.9. MFSP breakdown based on process area for integrated HTL with MEC with different scales

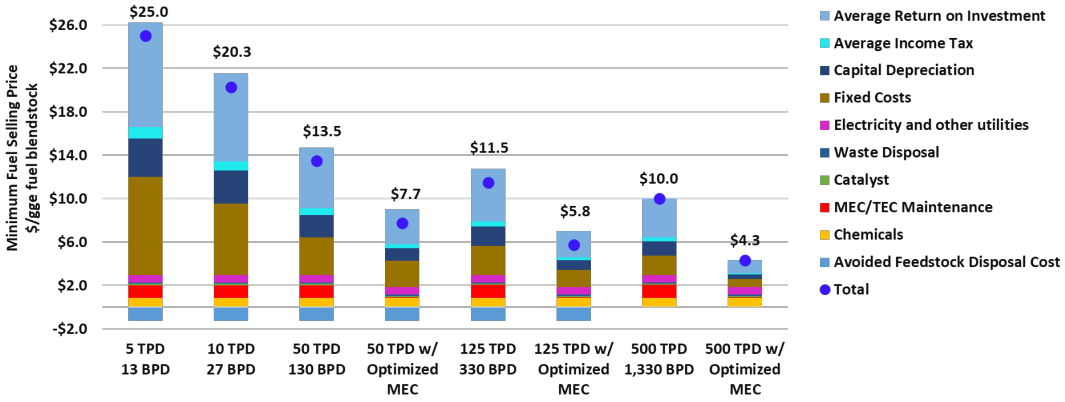

Figure 6.10. MFSP breakdown based on CAPEX and OPEX for integrated HTL with MEC with different scales

When compared to AD, as shown in **Figure 6.11**, the LCOD for Integrated System with Optimized MEC begins to compete with AD (to raw biogas) > 50 TPD scale. Specifically, for a larger plant scale (125 TPD plant), with optimized MEC component pricing, and the Biofuel price of $4/GGE, the HTL/MEC can achieve negative disposal cost, reducing the disposal cost by 119% compared to the AD disposal cost (Scenario 3).

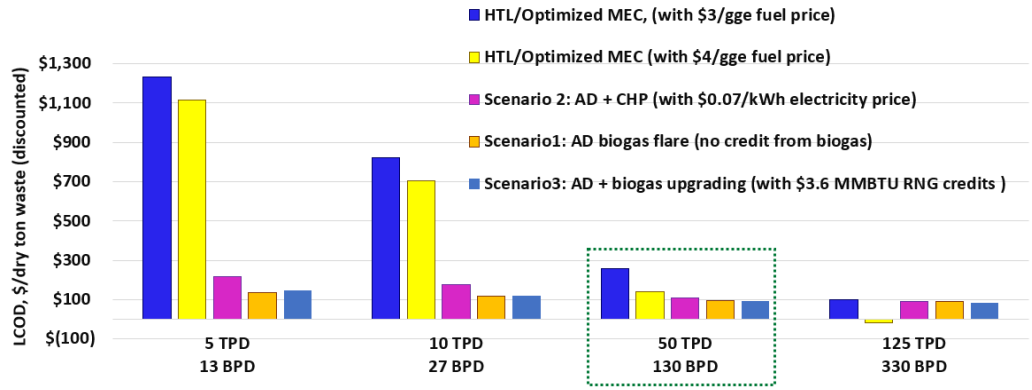

Figure 6.11. LCOD for Integrated System with Optimized MEC vs. AD

Task 6. LCA and System Analysis (Lead: Princeton Maravelias group)

Using an optimization model, we designed an integrated system that combines one HTL and one upgrading unit with three T-MEC units (see Figure 6.12). This optimized system requires the same total volume for the three MEC units but leads to the production of a cleaner treated water stream, leading to credits.

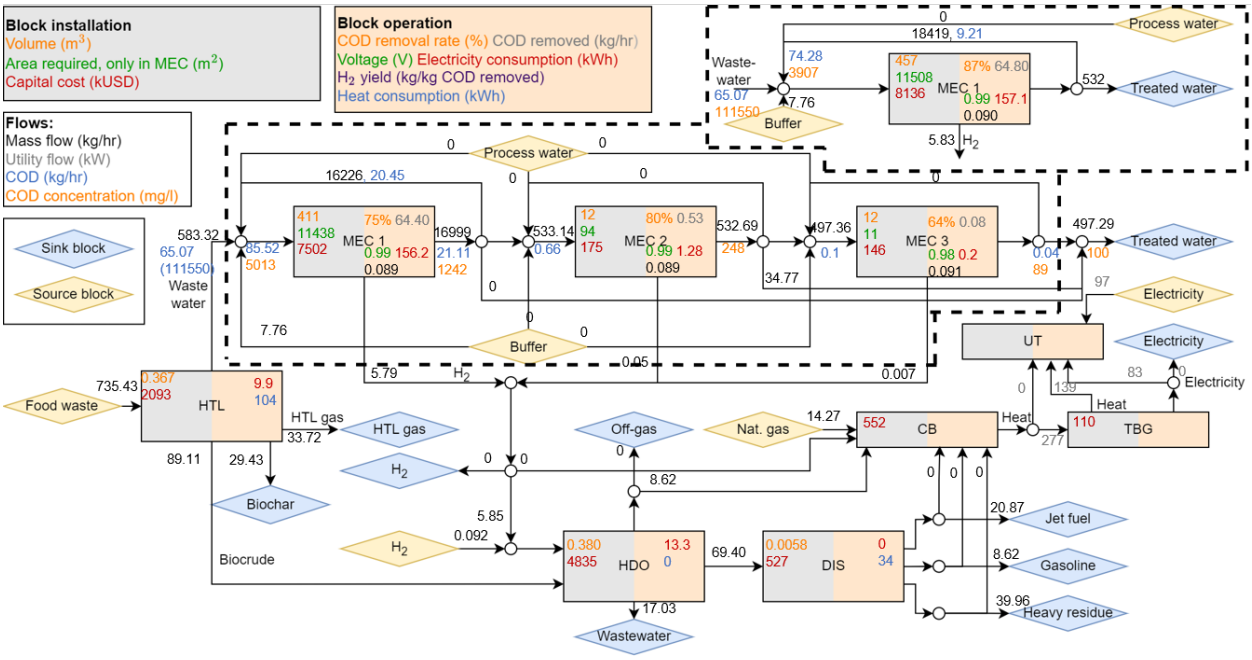

Figure 6.12: Block flow diagram of optimized system, basis: 5MT/day of food waste treated. Block abbreviations: HTL: hydrotreating, HDO: upgrading, DIS: distillation system to product separation, CB: boiler, TBG: turbogenerator, UT: utility plant.

Next, we performed life-cycle assessment for three distinct systems: (1) anaerobic digestion, (2) HTL coupled with upgrading, and (3) the proposed system (HTL with upgrading and three T-MEC units). The analysis was performed using *LCA for Experts* (formerly known as GaBi). The block flow diagrams of the three systems are shown in Figure 6.13.

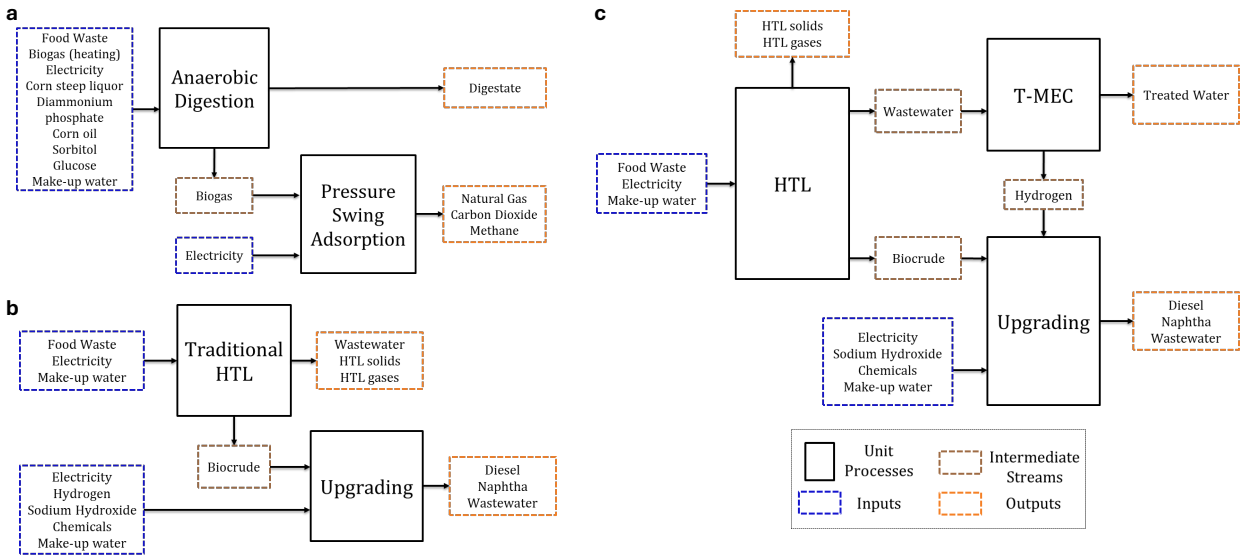

Figure 6.12: Systems considered for LCA: (a) anaerobic digestion, (b) HTL with upgrading, and (c) HTL with upgrading and T-MEC. Major inputs (in blue blocks) and outputs (in orange blocks) also shown.

If a typical 2024 grid electricity mix is used, the proposed system has higher global warming potential (GWP). However, as electricity becomes more renewable, the GWP of the proposed system will decrease faster, and it will reach parity with AD if renewable electricity is used. Also, we found that if the objective function of the design is the minimization of emissions, then the proposed system can yield better designs. Representative results, in terms of GWP, are given in Figure 6.13, while more detailed results, for three metrics (ecotoxicity, eutrophication potential, and GWP), are given in Figure 6.14.

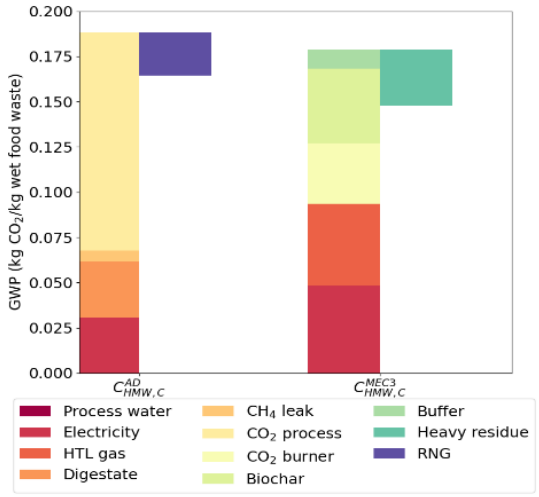

Figure 6.13. Contributors to GWP of anaerobic digestion ($C^{AD}_{HMW,C}$) and proposed system ($C^{MEC3}_{HMW,C}$).

We observe that the proposed system using three MEC units has improved performance compared to previous solutions because it requires less process water and has smaller electricity consumption. Also, the proposed system is better in terms of ecotoxicity & eutrophication.

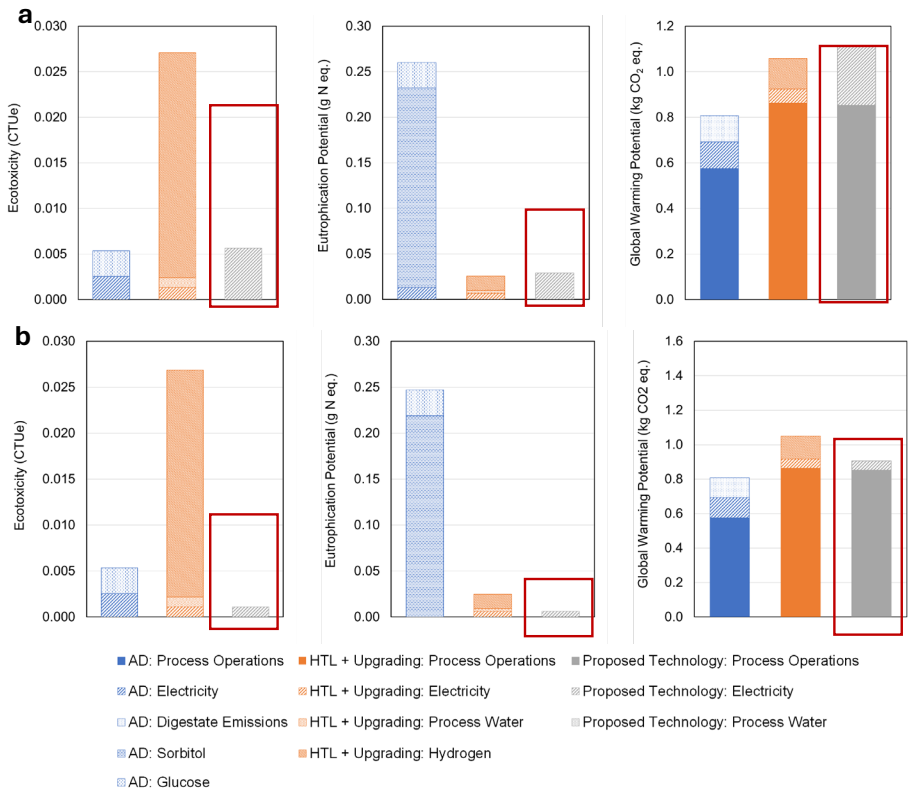

Figure 6.14. Environmental comparison, in terms of three metrics using the current electricity grid (panels a) and renewable electricity (panels b).

Figure 6.15 shows an energetic comparison between the AD and the proposed system under two different scenarios. The proposed system yields more energy (liquid fuel) compared to the renewable natural gas yield from AD but it requires more energy input for heat and power supply.

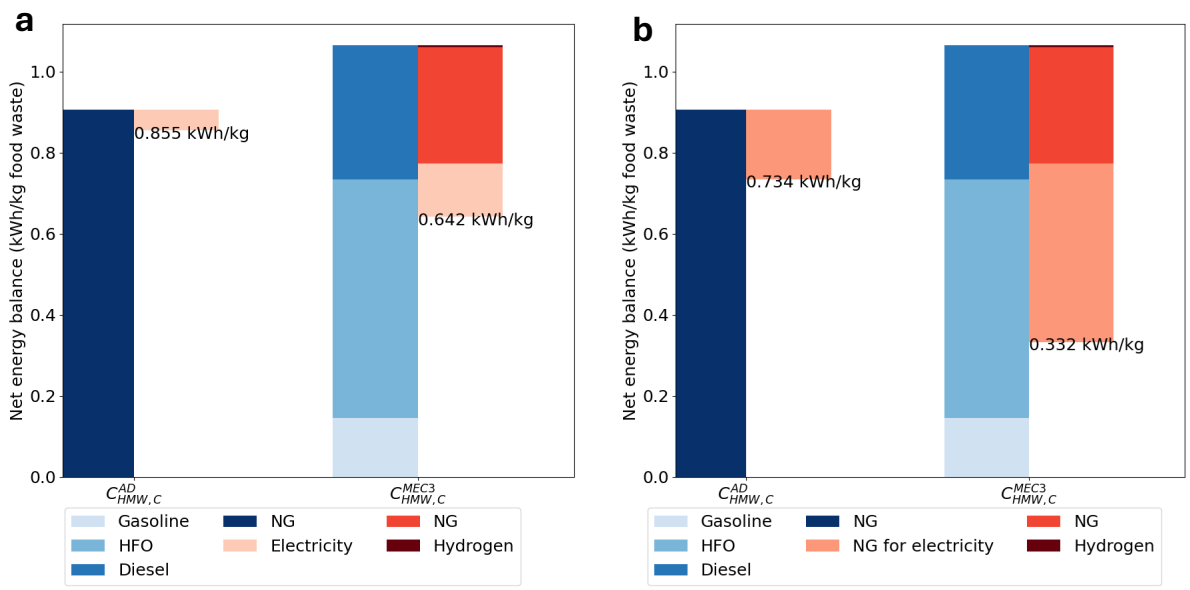

Figure 6.15. Energetic comparison of anaerobic digestion ($C^{AD}_{HMW,C}$) and proposed system ($C^{MEC3}_{HMW,C}$) when electricity is used directly (a) and when natural gas is used to generate electricity (b).

Finally, Figure 6.16 shows a comparison between AD combined with pressure swing absorption, for biogas purification, against the proposed system in terms of carbon efficiency. Table 6.9 gives carbon efficiencies for the two systems under different scenarios. We note that when renewable electricity is used, the proposed system has 60% higher efficiency.

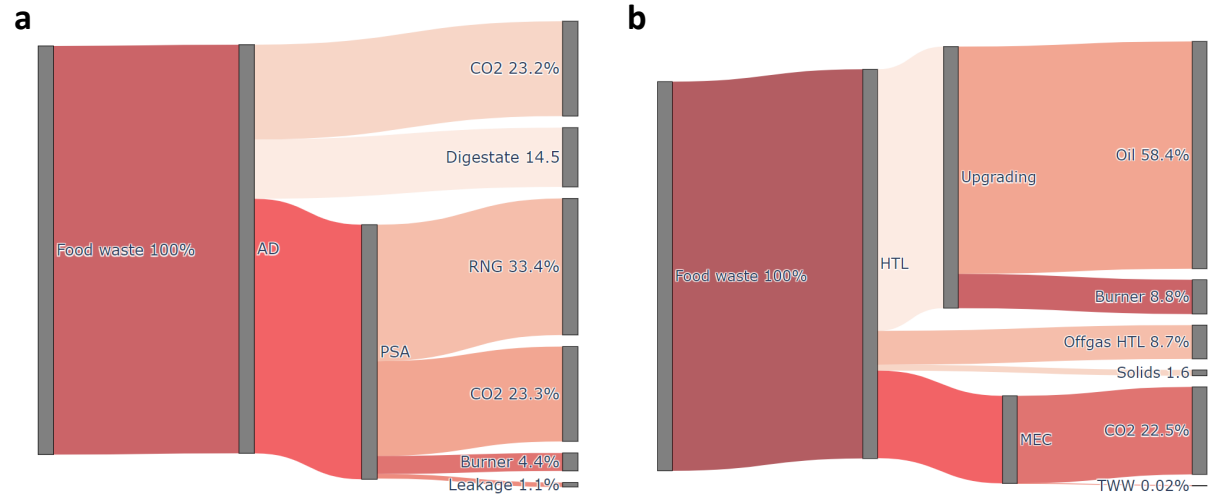

Figure 6.16. Carbon efficiency comparison: Shankey diagrams.

Table 6.9. Carbon efficiency comparison.

Carbon efficiency (%)	HTL + MEC	AD + PSA

Base line system: food waste to product	58	33
Considering renewable electricity and NG for heating	53	33
Considering NG for electricity and heating	47	31

8. Significant Accomplishments and Conclusions:

The project successfully met all milestones and targeted goals. The synergistic thermo-microbial-electrochemical (T-MEC) process was developed and piloted using actual food waste, biocrude oil and kerosene were produced, and PHW was treated with pilot MECs with sufficient H2 produced. System analysis shows the T-MEC successfully improves the carbon yield by >50% compared to the anaerobic digestion baseline and decreased the waste processing cost by >25% compared to AD.

The HTL pilot reactor processed food waste at a feed rate of 90 kg/h, achieving the capacity to produce up to 200 L of biocrude oil per day. The biocrude oil had high conversion efficiency, with SDW feedstock exceeding the mass yield goal and meeting the carbon efficiency goal. Besides water and ash removal, it was found that a wash step for desalting played a critical role in the pretreatment of HTL biocrude oil to avoid catalyst plugging and deactivation during hydrotreating. 100% deoxygenation and denitrogenation of the biocrude oil was achieved through parameter screening and optimization using cobalt molybdenum on alumina, meeting the >80% deoxygenation goal. The sulfur content of the biocrude oil was also reduced to <15 ppm, meeting the ASTM specification limit. Lastly, Tier α tests of the kerosene cut from upgraded HTL biocrude oil showed that it met important bulk properties of jet fuel, making it a good candidate for sustainable aviation fuel.

Both lab and pilot scale MECs were developed and characterized by using synthetic wastewater and actual PHW from HTL. The reactors achieved rapid startup times, biofilm formation, and effective operation. The lab reactors and analyses revealed degradation conversion pathways of major organic and nitrogen contaminants in PHW during MEC treatment, and a metabolic network was constructed to provide insights for enhancing treatment efficiency. Using a tiered voltage strategy in series, COD removal efficiency from the pilot reactor using actual PHS peaked at 86.4%, with H_2 production rates reaching 1.8 L H_2/L_{cat}/day - the highest recorded for pilot MECs of comparable size. In-parallel operation exceeded theoretical H_2 yield thresholds, achieving 0.127 kg H_2/kg COD, demonstrating the potential for on-site hydrogen production to support biocrude upgrading without external hydrogen inputs.

The team developed and evaluated cathodic materials for H_2 production from PHW using the TEC system. Both base metal and precious metal electrodes achieved 100 mmol H_2/(gmetal·h) production rates, with base metal showing cost-effective advantages due to lower molecular weight and comparable performance. Systematic tests demonstrated that buffer agents reduced energy consumption by up to 40%, and the

reactor could maintain stability over 120 hours. Additionally, the system demonstrated adaptability to different PHW compositions, maintaining consistent cathode performance while revealing the impact of anode stability on overall efficiency.

The TEA findings highlighted the HTL-MEC's potential for converting food waste into sustainable fuels. The results show the HTL-MEC achieved a carbon efficiency of 65% to biocrude and 58% to finished fuels (SAF, diesel, naphtha), significantly higher than AD's 41% and 33%, respectively. When optimized, the system's H_2 production from MEC could meet biocrude upgrading requirements without external inputs, while residual heat from HTL gas burning fully supported process energy needs. Scaling analysis revealed the minimum fuel selling price (MFSP) decreased from $25/GGE at a 5 tpd plant to $10/GGE at a 500 tpd scale, with economies of scale contributing to cost reductions. However, MEC costs remained a challenge due to a scaling factor of ~1.0. Optimizing MEC materials, including stainless steel cathodes, carbon fiber anodes, and cost-effective separators, reduced MFSP by $5.8/GGE across all scales. Sensitivity studies identified MEC current density, capital costs, and feedstock pricing as key drivers. For a 125 tpd plant with optimized MECs and a biofuel price of $4/GGE, the HTL-MEC system achieved negative disposal costs, reducing disposal costs by 119% compared to AD. This performance underscores the system's potential scalability, economic competitiveness, and optimization potential for sustainable biofuel production.

9. Path Forward:

The project demonstrated significant progress and potential in the development and pilot-scale implementation of the synergistic thermo-microbial-electrochemical (T-MEC) process for sustainable biofuel production. Moving forward, efforts will focus on reducing the cost of MEC materials, including membranes and electrodes, and improving performance through increased current densities and optimized operations. To mitigate deviances from properties of conventional jet fuel, an additional isomerization step could be implemented to convert linear alkanes into lightly branched alkanes. Additionally, research is needed to develop tailored systems and operational strategies for heterogeneous feedstocks and to integrate processes seamlessly for enhanced scalability and economic feasibility. With these advancements, the T-MEC process has strong potential to establish itself as a scalable and competitive technology for converting wet waste into sustainable fuels and products.

10. Products:

Publications

1. Summers, *et al.* (2023). Pilot-scale continuous plug-flow hydrothermal liquefaction of food waste for biocrude production. *Industrial & Engineering Chemistry Research*. https://doi.org/10.1021/acs.iecr.3c01587
2. Summers, *et al.* (2024). Multi-stage pretreatment of hydrothermal liquefaction biocrude oil as a precursor for sustainable aviation fuel production. *Fuel Processing Technology.* https://doi.org/10.1016/j.fuproc.2024.108118

3. Summers, *et al.* Food-fueled flight: Hydrothermal liquefaction pathway for drop-in sustainable aviation fuel. Under review.
4. Jiang, J., Lopez-Ruiz, J. A., Leininger, A., Du, L., Yan, Y., May, H. D., & Ren, Z. J. (2023). Molecular transformation and metabolic insights of microbial electrolysis treatment and valorization of post-hydrothermal liquefaction wastewater. *Green Chemistry*, *25*(22), 9115-9125. (Front Cover Article) https://doi.org/10.1039/D3GC02252H
5. Jiang, J., Lopez-Ruiz, J. A., Bian, Y., Sun, D., Yan, Y., Chen, X., ... & Ren, Z. J. (2023). Scale-up and techno-economic analysis of microbial electrolysis cells for hydrogen production from wastewater. *Water Research*, *241*, 120139. https://doi.org/10.1016/j.watres.2023.120139
6. Jiang, J., Du, L., Si, B., Kawale, H.D., Wang, Z., Summers, S., Lopez-Ruiz, J.A., Li, S., Zhang, Y. and Ren, Z.J., 2025. Pilot microbial electrolysis cell closes the hydrogen loop for hydrothermal wet waste conversion to jet fuel. Water Research, 268, p.122644. https://doi.org/10.1016/j.watres.2024.122644
7. Lopez-Ruiz, J.A., Riedel, N.W., Boruah, B., Bhatwadekar, S.S., Strange, L.E. and Li, S., 2023. *Low-temperature electrochemical wastewater oxidation* (No. PNNL-35535). Pacific Northwest National Laboratory (PNNL), Richland, WA (United States). https://doi.org/10.2172/2332860
8. Gutiérrez, O.Y., Grubel, K., Kothandaraman, J., Lopez-Ruiz, J.A., Brooks, K.P., Bowden, M.E. and Autrey, T., 2023. Using earth abundant materials for long duration energy storage: electro-chemical and thermo-chemical cycling of bicarbonate/formate. *Green Chemistry*, *25*(11), pp.4222-4233. https://doi.org/10.1039/D3GC00219E
9. Granacher, J., Franzoi, R., Jiang, J., Summers, S., Li, S., Lopez-Ruiz, J.A., Zhang, Y., Ren, ZY., Maravelias, CT. Drop-in fuel production from food waste: system level optimization and analysis, Journal of Cleaner Production, in review.

Presentations

1. Summers, S. et al., Pilot-scale hydrothermal liquefaction of wet biowaste", American Chemical Society 2023 Spring Conference, 2023.
2. Summers, S. et al., Toward a circular bioeconomy: Food waste to sustainable aviation fuel, Conference for Digital Agriculture, University of Illinois Urbana-Champaign, 2024.
3. Summers, S. et al., From food waste to sustainable aviation fuel via hydrothermal liquefaction and catalytic upgrading, INFEWS and Circular Bioeconomy Systems Workshop, University of Illinois Urbana-Champaign, 2024.
4. Summers, S. et al., Catalytic hydrotreating of hydrothermal liquefaction biocrude oil for sustainable aviation fuel, ASABE Annual International Meeting, 2024.
5. Zhang, Y. et al. Hydrothermal liquefaction pathway for decarbonization in the aviation sector", North American SAF Conference & Expo, 2024.
6. Jiang, J. et al. Molecular transformation and metabolic insights of microbial electrolysis treatment and valorization of post-hydrothermal liquefaction wastewater" Association of Environmental Engineering and Science Professors (AEESP) biennial research & education conference 2022

7. Jiang, J. et al. Pilot microbial electrolysis cell closes the hydrogen loop for hydrothermal wet waste conversion to jet fuel" American Chemical Society National Meeting Fall, 2023
8. Lopez-Ruiz, J., et al. Highlighting Startups Pursuing Electrochemical Manufacturing" Symposium organization for 245th ECS Meeting in San Francisco, CA, 2024
9. Li, S., et al. Techno-Economic Assessment of Food Waste to Biofuel By Integrated Hydrothermal Liquefaction with Microbial Electrolysis Cell (2023). AIChE Annual Meeting in Orlando, FL. 2023
10. Lopez-Ruiz, J., Hydrothermal Liquefaction of Biowaste into Biocrude and Reuse Nutrients – A Paradigm for Environment-Enhancing Food and Agriculture System, 2023.
11. Lopez-Ruiz, J., et al. Developing Electrocatalytic Processes for the Conversion of Biomass-Derived Molecules into Fuels and Chemicals at Normal Temperature and Pressure, Organic Reactions Catalysis Society, PNNL, 2023

Awards

1. National Science Foundation Graduate Research Fellowship, 2022, Sabrina Summers
2. Agricultural and Biological Engineering Graduate Student Research Excellence Award, 2023, Sabrina Summers
3. Grainger College of Engineering Mavis Future Faculty Fellow, 2023, Sabrina Summers
4. ARCS Illinois Foundation Scholar Award, 2023, Sabrina Summers
5. Agricultural and Biological Engineering Graduate Student Research Excellence Award, 2024, Zixin Wang
6. Spitze Land-Grant Professorial Career Excellence Award, College of Agriculture, Consumer and Environmental Sciences, 2024, Yuanhui Zhang
7. Best Student Poster Award AEESP 2022, Jinyue Jerry Jiang
8. Andlinger Center for Energy and the Environment 2023 Annual Meeting Graduate Presentation Award, Jinyue Jerry Jiang
9. Peter B. Lewis Fund for Student Innovation in Energy and the Environment, Jinyue Jerry Jiang
10. 2024 Maeder Graduate Fellowship in Energy and the Environment, Jinyue Jerry Jiang
11. National Lab Accelerator Pitch Event - November 16 in Palo Alto, CA with the pitched titled, "Cleaning Wastewater for Energy Production and a Sustainable Future." Juan Lopez-Ruiz
12. Reaching a New Energy Sciences Workforce (BES-RENEW) Program to increase participation of underrepresented groups in clean energy research. Juan Lopez-Ruiz

Inventions

- Invention Title: Molybdenum Carbide-zeolite-iron Nanocatalysts for Production of Sustainable Aviation Fuels from Biocrude Oils
- EIR Number: 0577704-24-0088

11. Project Team and Roles:

PI and Co-PIs:

PI: Zhiyong Jason Ren (Princeton) – Overall project management, MEC tasks
Co-PI: Juan Lopez Ruiz (PNNL) – TEC research, TEA task
Co-PI: Lesley Snowden-Swan (PNNL) – TEA task
Co-PI: Yuanhui Zhang (UIUC) – HTL task
Co-PI: Christos Maravelias (Princeton) – System analysis task

Postdocs and Students:

Shuyun Li – Research associate, performed the majority of the TEA analysis
Sabrina Summers – PhD student (female), National Science Foundation Graduate Research Fellow, is focus on upgrading the HTL biocrude from food waste into jet fuel.
Zixin Wang -- PhD student (female), Graduate Research Assistant, is focus on characterization of food waste and treatment of the post-HTL wastewater.
Jerry Jiang – PhD student, focusing on reactor development and characterization
Yuqing Yan – PhD student, molecular microbiology analysis
Aaron Leininger – PhD student, reactor development
Julia Granacher – Postdoc, LCA and system analysis
Robert E. Franzoi Junior - Postdoc, LCA and system analysis

Undergraduate Research Assistants

Siyu Yang -- Undergrad RA (female), assists on upgrade biocrude
Lane Weber -- Undergrad RA, assisted on food waste pretreatment and HTL operation
Senior Capstone Design Team: work on upgrading HTL reactor data and control system
Dev Kothari -- CS Senior, focus on MATLAB programming
Akshay Dugar -- ME Senior, Focus on control system design
Alice Lin -- ME Senior (female), focus on data acquisition
Luren Wang -- ME Senior, focus on interfacing and dashboard presentation
Qianxi Kong -- ME Senior (female), focus on control system integration
Leila Owens – CEE Senior (female), focus on water electrolysis analysis

12. References:

1. Summers, S., Valentine, A., Wang, Z. & Zhang, Y. Pilot-Scale Continuous Plug-Flow Hydrothermal Liquefaction of Food Waste for Biocrude Production. Ind Eng Chem Res (2023) doi:10.1021/acs.iecr.3c01587.
2. Aierzhati, A. et al. Development of a mobile, pilot scale hydrothermal liquefaction reactor: Food waste conversion product analysis and techno-economic assessment. Energy Conversion and Management: X 10, 100076 (2021).

3. Ghadge, R., Nagwani, N., Saxena, N., Dasgupta, S. & Sapre, A. Design and scale-up challenges in hydrothermal liquefaction process for biocrude production and its upgradation. Energy Conversion and Management: X 14, 100223 (2022).
4. Watson, J. et al. Towards transportation fuel production from food waste: Potential of biocrude oil distillates for gasoline, diesel, and jet fuel. Fuel 301, 121028 (2021).
5. Taghipour, A., Ramirez, J. A., Brown, R. J. & Rainey, T. J. A review of fractional distillation to improve hydrothermal liquefaction biocrude characteristics; future outlook and prospects. Renewable and Sustainable Energy Reviews 115, 109355 (2019).
6. Xin, Q., Alvarez-Majmutov, A., Dettman, H. D. & Chen, J. Hydrogenation of Olefins in Bitumen-Derived Naphtha over a Commercial Hydrotreating Catalyst. Energy and Fuels 32, 6167–6175 (2018).
7. Mäki-Arvela, P., Kaka khel, T., Azkaar, M., Engblom, S. & Murzin, D. Catalytic Hydroisomerization of Long-Chain Hydrocarbons for the Production of Fuels. Catalysts 8, 534 (2018).
8. Yang, Z. et al. A GC × GC Tier α combustor operability prescreening method for sustainable aviation fuel candidates. Fuel 292, (2021).
9. Heyne, J., Rauch, B., Le Clercq, P. & Colket, M. Sustainable aviation fuel prescreening tools and procedures. Fuel 290, 120004 (2021).
10. Voigt, C. et al. Cleaner burning aviation fuels can reduce contrail cloudiness. Commun Earth Environ 2, (2021).
4. Jiang, J. et al. Molecular transformation and metabolic insights of microbial electrolysis treatment and valorization of post-hydrothermal liquefaction wastewater. Green Chemistry, 25(22), 9115-9125. (2023).
5. Jiang, J. et al. Scale-up and techno-economic analysis of microbial electrolysis cells for hydrogen production from wastewater. Water Research, 241, 120139. (2023).
6. Jiang, J. et al. 2025. Pilot microbial electrolysis cell closes the hydrogen loop for hydrothermal wet waste conversion to jet fuel. Water Research, 268, p.122644. (2025).